Effects of Micro Cellulose Fibers Addition on Concrete Mechanical Properties Under Flexure and Uniaxial Tension

by

Nouman Zubair
Bachelor of Sciences in Materials Engineering, GIK Institute Pakistan, 2011

A Report Submitted in Partial Fulfillment
of the Requirements for the Degree of

MASTER OF ENGINEERING

in the Department of Mechanical Engineering

Supervisory Committee

Effects of Micro Cellulose Fibers Addition on Concrete Mechanical Properties Under Flexure and Uniaxial Tension

by

Nouman Zubair
Bachelor of Sciences in Materials Engineering, GIK Institute Pakistan, 2011

Supervisory Committee

Dr. Rishi Gupta, (Department of Civil Engineering)
Supervisor

Dr. Caterina Valeo, (Department of Mechanical Engineering)
Departmental Member

Abstract

Natural fiber reinforced concrete (NFRC) has been brought into the lime light again by researchers to address the issues of sustainability, recyclability, and CO_2 gas emission that are associated with the manufacturing and usage of construction materials. As fibers are one of the main ingredients of NFRC, understanding their effect on the mechanical properties of the concrete requires much attention to provide users a confidence to use more sustainable materials in construction.

In this study, processed virgin micro cellulose fibers extracted from pine trees were added in 32 MPa concrete in two different volume fractions i.e. 0.25% and 0.5%. As compressive strength and tensile strength are important design parameters that need to be accounted for in structural design applications, these strengths were evaluated using applicable ASTM standards after 28 days of wet curing. Owing to inherent difficulties in testing concrete under direct tension, the flexural test was employed to determine the tensile properties through inverse analysis of the concrete under consideration. An effort was also made to test the equivalent strength mortar in direct tension and report the difference in tensile properties generated from the indirect test (flexural) and the direct uniaxial tension test. It was observed that the addition of 0.25% fiber V_f in concrete caused the most increase in peak load which was followed by 0.5% fiber V_f. Decrease in peak load capacity with an increase in fiber volume fraction was attributed to the poor dense structure that resulted because of fiber mixing issues in concrete.

Supervisory Committee
Dr. Rishi Gupta, (Department of Civil Engineering)
Supervisor
Dr. Caterina Valeo, (Department of Mechanical Engineering)
Departmental Member

Table of Contents

List of Tables

List of Figures

Acknowledgments

I am much indebted to Dr. Rishi Gupta for his unwavering support of me during my study period, making it possible for me to finish my degree with comfort and ease. A special thanks to Dr. Armando Tura and his team in facilitating research activities and taking care of last minute requests. Also, an acknowledgment of Harsh Rathod's guidance on Close loop testing which would not have been possible to conduct on my own.

Dedication

To my parents, who have taught me to remain resilient in the face of difficulties and always backed me in achieving my dreams. This degree would not have been possible without their emotional and financial support.

1 Introduction

1.1 Background

As the worldwide demand of infrastructure development has gone up owing to an increase in the worlds population, the construction industry nowadays is looking for more sustainable ways to reduce reliance on traditional construction materials made by extensive energy demand processes. Manufacturing of these materials also has a major impact on greenhouse gas emission, so the construction industry is looking to cater to the environmental effects of these materials by increasing the use of green materials in construction. World Commission on Environment Development has defined sustainability as “meeting the needs of present without compromising the ability of future generations to meet their own” [1]. To support the idea of sustainable construction and usage of green materials, the use of renewable materials and industrial by products in construction is the need of the hour.

Presently, the use of fibers in concrete is quite popular owing to their proven performance. Since past few decades, extensive research has been carried out to study the effect of fiber addition on concrete where it became evident that crucial properties of concrete like tensile strength, impact resistance, toughness, and ductility etc. can be remarkably improved by adding the right amount and type of fibers to it [2]. Keeping in view the current research trends in the field of construction, this study is aimed at evaluating the performance of micro cellulose fibers in concrete under flexure and uniaxial tension loads.

1.2 Problem statement

Micro cellulose fibers present a class of natural fibers that fall under the category of specialty fiber [2]. Although much of the experimental studies conducted by researchers are regarding processed macro natural fibers in concrete, not much experimental data is available for specialty fibers performance in concrete under flexure and tension.

1.3 Objective

This study aims at understanding the effects of micro cellulose fiber addition in concrete under flexure and tension loads by using different fiber volume fractions, thus identifying the optimal fiber volume fraction that positively impacts the mechanical performance of the concrete. Furthermore, attempt is made to correlate the back calculated tensile properties, generated through flexural test, with the direct tension test tensile properties.

1.4 Approach

This report begins with the literature review on the fiber reinforced concrete regarding natural fibers where the general properties of these fibers in listed and their effect on mechanical properties of concrete is highlighted. This is followed by the description of the experimental program employed in this study which highlights the mixture proportion development, material information, and tests setup. Chapter 4 discusses the results and analyzes the effects of fiber addition on concrete as per the objective of the study. Lastly, recommendations are laid down in the conclusion section and future work is also proposed.

2 Fiber Reinforced Concrete

2.1 Introduction

According to the ACI 116R [3], fiber reinforced concrete (FRC) is defined as the concrete containing randomly oriented dispersed fibers. These fibers provide reinforcement to the brittle cement matrix and helps in improving ductility which is especially noticeable in post peak response of the load-deflection curve. Moreover, different types of fibers are added into the cementitious matrix that helps in improving the low tensile strength, low strain ability at fracture, elastic modulus, fracture toughness, fatigue, shrinkage, and durability. These fibers have been categorized into four major categories as per ACI 544.1R [4] and include steel fiber, synthetic fibers, glass fibers, and natural fibers.

Fibers from any of the four major categories are used in short and discrete form and are randomly distributed throughout the matrix. Volume fraction of fibers directly impact the post crack behavior as more percentage tends to increase the ductility but at the expense of the workability. Fig-1 illustrates the concept of fiber addition in concrete;

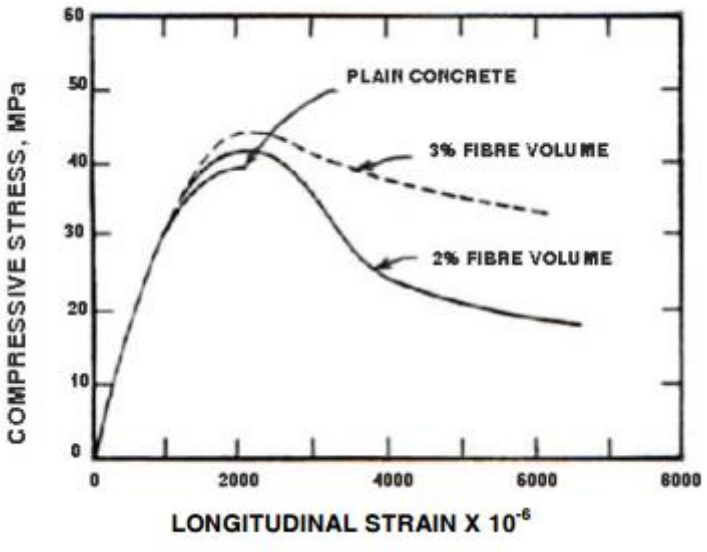

Figure 1 - Effect of fibers addition on plain concrete [5]

Moreover, the actual effect of these fiber additions depends on various factors that include fibers type, geometry, size, distribution, and volume fraction.

Failure of FRCs starts from tensile cracking of the matrix on planes where normal tensile strains surpasses the allowed values. If the fibers are sufficiently long, or high performance, extensive cracking normally occurs in the matrix prior to complete failure of composite. However, in the case of short and discrete fibers like steel, polypropylene, glass, or natural fibers once the matrix is cracked the following type of failure may occur [6];

a) After matrix cracking, composite fracture immediately may occur due to;

i. Inadequate fibers quantity at the critical section or

ii. Insufficient fiber L_c that could not transfer the tensile stress throughout the matrix

b) After matrix cracking, FRCs continue to carry the load but at decreasing rate, also called strain softening. This results in increase in toughness but tensile strength remains the same.

c) After matrix cracking, FRCs continues to carry the increasing load thus resulting in peak stress and corresponding deformation greater than that of matrix alone.

By looking at the above failure modes, (c) is desirable as it leads to increase in both tensile strength and toughness of the concrete. This failure mode is characteristic behavior of high performance fiber reinforced concrete composites (HPFRCC). Understanding of these failure modes is important as it gives the indication of the FRCs limitation. Fig-2 illustrates the failure mode stated above;

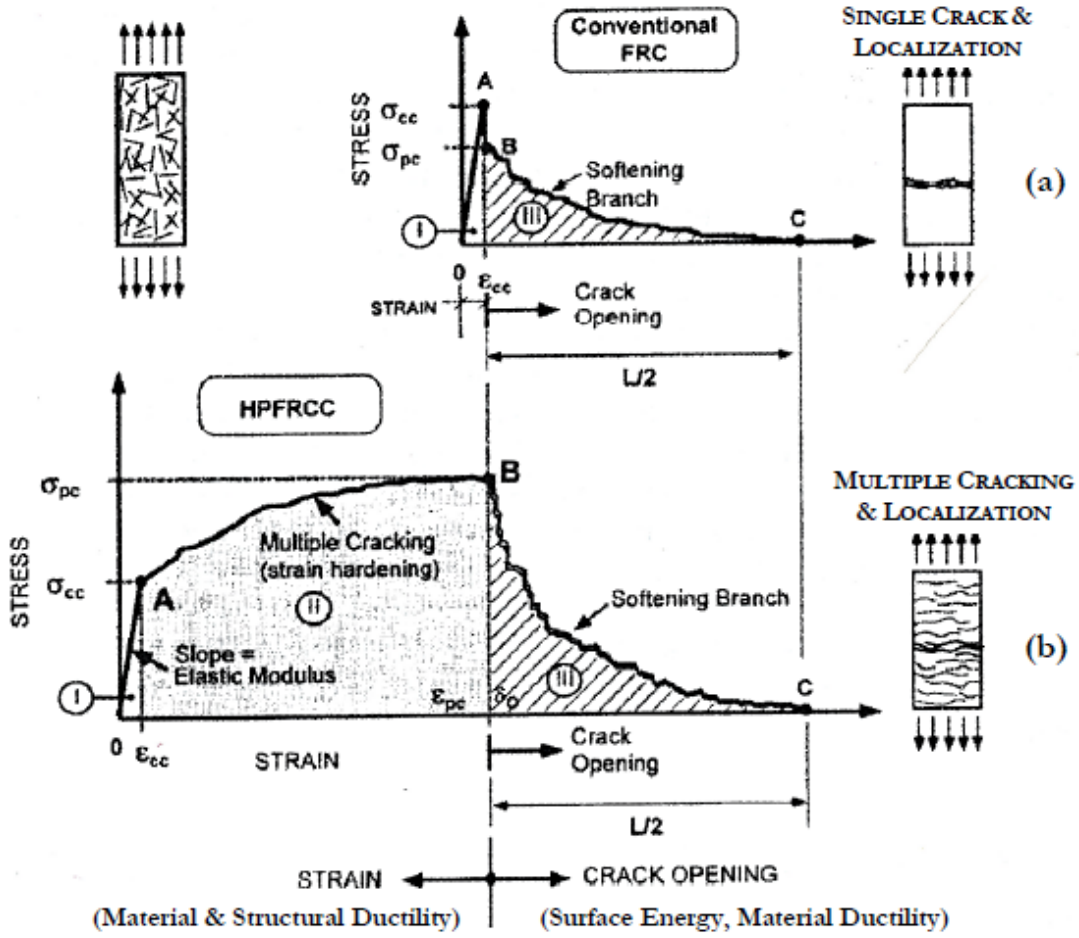

Figure 2 - Stress-strain behavior of different FRCs [7]

2.2 Natural Fiber reinforced concrete

2.2.1 Overview

Recently, much of the research is being conducted in the field of natural fiber reinforced concrete (NFRC) to further understand the durability and mechanical aspects of natural fiber addition in concrete. Many aspects of fiber addition are being considered by researchers out of which one important aspect is to understand the use of micro scale specialty fibers in concrete. Specialty fibers (also called speciality cellulose fibers) are processed plant based natural fibers that are chemically treated to enhance alkali

resistance and bond enhancement in concrete matrix. To better understand the effect of micro cellulose fibers addition in concrete, the literature review section is divided into two parts; the first part gives an insight into effects of natural fibers addition in concrete whereas the second part sheds light on the effects on micro scale fibers on concrete. Lastly, an experimental work carried out by Banthia et al. [16] is presented in which micro cellulose fibers were used as a reinforcement.

2.2.2 Natural Fibers as reinforcement

As the term implies, concrete when reinforced with natural fibers is referred to as natural fiber reinforced concrete (NFRC). Since the focus of academia and the industry is on reducing greenhouse gas emissions associated with concrete, natural fibers have been a center of focus because of their notable characteristics of being eco-friendly and recyclable. Most of the natural fibers used in concrete are vegetable or wood fibers that are widely available throughout the world at a much cheaper rate compared to other fiber types. Table-1 highlights the cost advantage that natural fibers offer;

Fiber type		**Price (USD/m^3)**
Steel		7110- 11850
Glass		3250 – 5000
Synthetic	Polypropylene	1620 – 2700
	Polyethylene	1380 – 2300
Natural	Sisal	750
	Banana	800
	Coir	600

Table 1 - Comparison of prices (USD) for different types of fiber [8]

As natural fibers can be used in unprocessed and processed states, it’s imperative to understand the composition and the source of its strength.

Natural fibers have a specific composition and are regarded as cellular structures. Usually, cellulose, hemicellulose, lignin, and pectin are the main constituents of natural fibers structure. Fig-3 depicts a typical structure of natural fibers.

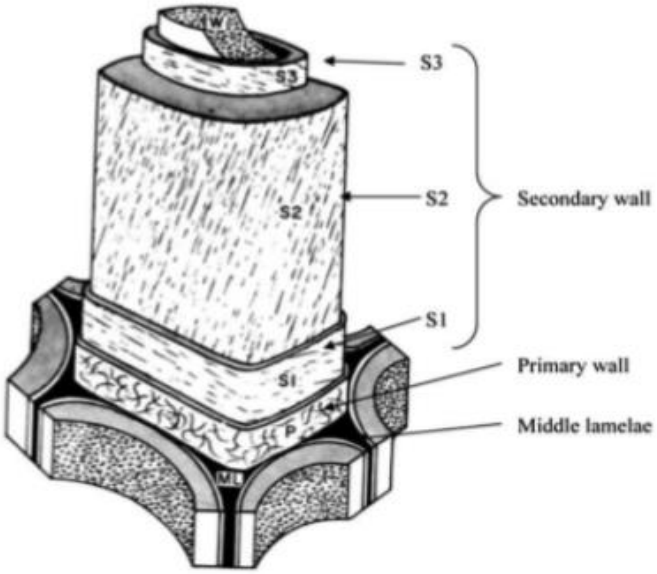

Figure 3 - Structural schematic of natural fibers [8]

Complete structure of natural fibers is composed of several layers that are made up of cellulose fibrils in the matrices of proteins, lignin, and hemicellulose [9], [10].

Natural fiber strength and stability comes from cellulose which is a linear polymer unit consisting of glucose chains. When exposed to an acidic environment, cellulose is easily hydrolyzed into water soluble sugar, whereas it is resistant to strong alkalis. Compared to cellulose, hemicellulose is a branched polymer and has little contribution in strength and stiffness of fibers. Also, hemicellulose is hydrophilic in nature and offers no resistance to acidic and alkali environments. The source of compressive strength and stiffness of natural fibers is lignin, which is a heterogeneous mixture of phenyl propane monometers and aromatic polymers [9].

To improve the durability aspect of natural fibers used in concrete, fibers are processed to make them alkali resistant. If not treated for an alkali environment, lignin in natural fibers

is decomposed and leads to significant degradation of mechanical properties of NFRC. Processes employed to make them alkali resistant includes acidic, alkali, or pyrolysis treatments. Tables 2 and 3 illustrate the composition of commonly used natural fibers and their associated mechanical properties;

Fiber	Cellulose (wt%)	Hemicellulose (wt%)	Lignin (wt%)	Wax (wt%)
Abaca	45.4	38.5	14.9	2
Bamboo	26 - 43	30	21 - 31	-
Coir	33.2 - 43	31.1	20.5	-
Cotton	85 - 90	5.7	-	0.6
Flax	64.1 - 71	16.7 – 20.6	2.0 – 2.2	1.5
Sisal	33.4 - 78	10 – 24	9.9 – 22.7	0.3 - 2

Table 2 - Composition of different types of natural fibers [11]

Fiber	Density (g/cm3)	Elongation (%)	Tensile Strength (MPa)	Young's modulus (GPa)
Abaca	1.5	3 – 10	400	12
Bamboo	0.6 – 1.1	-	140 – 230	11 – 17
Coir	1.2	15 – 30	175 – 220	4 – 6
Cotton	1.5 – 1.6	3 - 10	287 – 597	5.5 – 12.6
Flax	1.4 – 1.5	1.2 – 3.2	345 – 1500	27.6 – 80
Sisal	1.33 – 1.5	2.0 – 2.5	400 – 700	9 - 22

Table 3 - Mechanical and physical properties of different types of natural fibers [11]

It has been shown in various experimental studies that the addition of natural fibers contributes to the enhancement of ductility, toughness, and impact resistance of the

concrete [2], [4]. Furthermore, significant impact of moisture content on mechanical properties of NFRC is also reported by researchers. In one of the study by Coutts et al. [12] it was presented that hydrogen bonding between fibers, and between fiber and matrix is significantly deteriorated by the increase in water absorption. In another study carried out by El-Ashkar et al. [13], it was reported that the failure mode of NFRC specimens is effected by the presence of moisture content. In this study, wet cured specimens showed an overall increase in the toughness value as compared to over dried specimens where increase in flexural strength was noted.

2.2.3 Micro fibers as reinforcement

Shah et al. [14] reported the effects of fiber size on mortar mechanical properties. Direct tension tests were carried out on ten batches of PVA fiber reinforced mortar with fiber volume fractions of 1%,2%, and 4%. It was noted that short fibers were more efficient in increasing the magnitude of first peak stress. They were able to bridge the micro cracks preventing them from transforming into macro cracks. Fig-4 depicts the general effect of fiber size on concrete response. In another study carried out by Banthia et al. [15], fibers synergy in high strength concrete matrices was evaluated. It was noted that micro fibers when used in conjunction with macro fibers in optimal volume fractions led to an overall improvement in toughness. This improvement is a result of the ability of micro fibers to bridge micro cracks and stop them from merging into macro crack. Once macro crack is formed, its propagation is hindered by macro fibers.

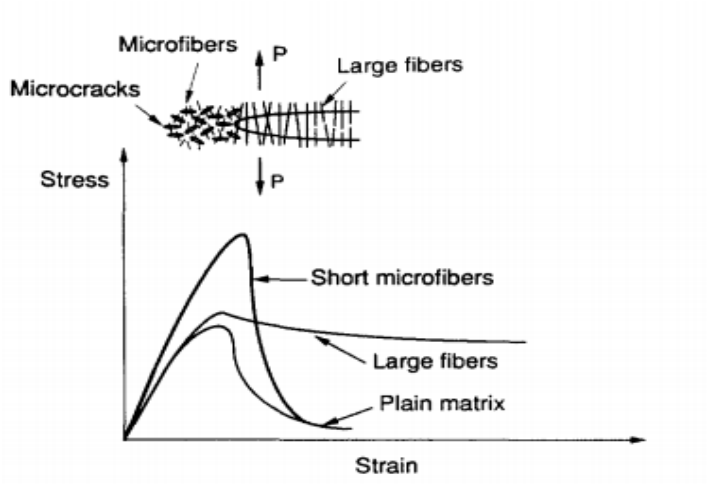

Figure 4 - Effects of different sizes of fibers on crack bridging [14]

2.3 Micro cellulose fibres as reinforcement

Banthia et al. [16] studied the effects of hybrid fiber, including micro cellulose fiber, addition in concrete under flexure and direct shear. The aim of the study was to find the best hybrid mix from a given set of fibers to determine fiber synergy. Along with micro cellulose fibers (C), two different types of steel fibers, hooked end (HE) and double deformed (DD), were used in the study. Ten design mixes were cast that included plain concrete, three design mixes with each type of fiber and the remaining six design mixes used a combination of all three fiber types with varying volume fraction. Micro cellulose fibers were used in 0.5% volume fraction, whereas other two fiber types were used in 0.3% and 0.5% volume fraction. It was observed that micro cellulose fiber addition had little effect on compressive strength of concrete, whereas 0.5% cellulose fiber with 0.5% hooked end steel fiber had a maximum effect on concrete strength, causing it to increase from 56 MPa to 61 MPa. Other combinations of fibers in concrete had either nominal or no effect on concrete compressive strength. Similarly, design mixes were subjected to flexural tests where micro cellulose fibers had shown minimal/no effect on improving post crack strength of concrete. Combination of 0.5% cellulose and 0.5% hooked end steel fibers had caused the concrete to show a strain hardening response in post crack region. Flexural graphs from this experimental study are presented in Fig 5 and 6.

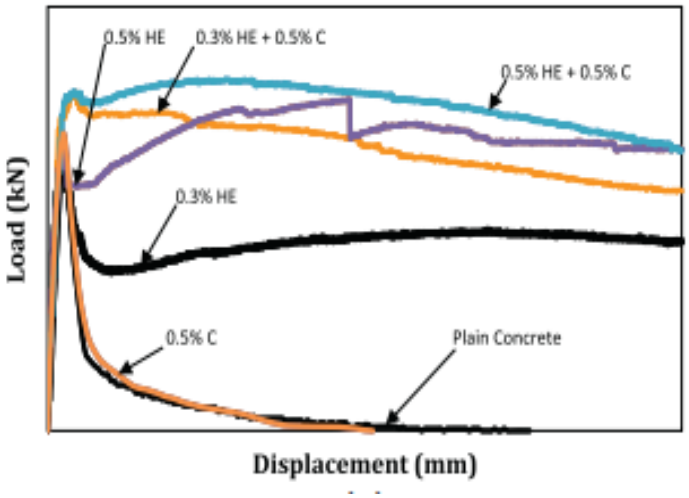

Figure 5 - Load vs Deflection response of hybrid HE & C fibers [15]

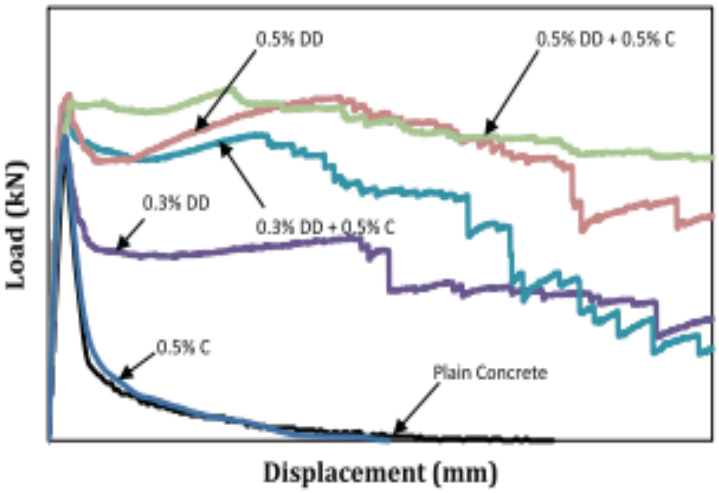

Figure 6 - Load vs Deflection response of hybrid DD & C fibers [15]

Similarly, micro cellulose fibers had not shown any effect on shear strength of concrete. It was concluded in the study that the lone addition of cellulose fibers of micro scale had little/no effect on concrete properties, where as hybrid mix of micro cellulose fibers and hooked end steel fibers had shown a positive synergy in all instances.

3 Experimental Program

3.1 Introduction

As outlined before, one of the objectives of this project was to correlate uniaxial tensile properties of FRC with its flexural properties. However, owing to the unavailability of the required testing equipment, uniaxial tension tests on concrete could not be performed, but an attempt was made by selecting an appropriate equivalent concrete strength mortar and testing it under uniaxial tension testing. In doing so, an assumption was made that mortar under tension would behave the same way as concrete under tension. Hence, to achieve the required objectives of the project, two types of materials were worked on i.e. concrete under flexure and mortar under uniaxial tension.

Experimental work was initiated with the selection of strength class of concrete and mortar. 32 MPa strength class was selected for the concrete. The subsequent step was to select the appropriate volume fraction of specialty cellulose fibers that were to be used in the project. Fiber volume fraction of 0%, 0.25%, and 0.5% were selected for a parametric study for this project. This range of volume fraction was selected based on the literature survey where researchers have used this range as the basis of their study [16], [17].

3.2 Materials Properties

The following sections detail the types and associated properties of constituent materials of concrete and mortar

3.2.1 Cement and aggregates

Aggregates used in the project were obtained from the Sechelt pit in B.C. Coarse, and fine aggregates had a relative dry density of 2.695 and 2.651 respectively, associated absorption ratio of 0.69% and 0.79%. Nominal size of coarse aggregates was 12.5mm. All this data is reflected in analysis reports provided by the supplier and attached in appendices A-I, A-II, and A-III respectively. Type 10 general use Ordinary Portland Cement (OPC), as per ASTM C150 [18] specifications, was used in the making of concrete and mortar samples.

3.2.2 Fibers

Fibers used in this study were obtained from Solomon Colors, INC. which manufactures a special type of natural cellulose fiber called UltraFiber 500 made from Loblolly and Slash pines in North America. As per manufacturer's claim, UltraFiber 500 is an alkali resistant cellulose based micro fibers used for secondary reinforcement of concrete. Close view of fibers is shown in Fig-7.

Figure 7 - Micro cellulose fibers

Studies carried out with this specific type of fiber have shown to improve the impact resistance, freeze/thaw resistance, and durability of concrete without having adverse effects on finishability or appearance of concrete [19], [20], [21]. Use of these natural cellulose fibers in concrete also supports the idea of sustainability as they come from natural renewable sources, thus making them environmentally friendly. General properties of the fibers are listed in table 4.

Fiber name	"Solomon UltraFiber 500"
Material type	Alkali-resistant, natural cellulose fibers
average length	2.1 mm (0.083 inch)
average denier	2.5 g/9,000m
average diameter	0.00063 inch
density	1.10 g/cm^3
tensile strength	750 N/mm^2
average elastic modulus	8,500 N/mm^2

Table 4- General properties of UltraFiber 500 [22]

3.3 Mixture proportion development

3.3.1 Concrete mix design

After selection of strength class and material types, the next step was to select the optimum mix design ratio for concrete that would produce the required properties. Cement/sand ratio and water/cement ratio were selected as 0.41 and 0.53 respectively.

Three types of concrete mix designs were formulated, as micro fibers were used in 3 different quantities. These mix designs were labelled as CCxx, 0.25%Cxx, and 0.5%Cxx, where CC refers to control concrete i.e. 0% fibers, percentage fraction in remaining two mix design indicate fiber volume fraction used in that mix design, C refers to concrete, and xx refers to sample identification number e.g. 0.25% C01 indicates sample #1 for 0.25% concrete mix design. Mix proportion used for concrete is listed table 5.

Cement	340	Kg/m^3
Aggregate	1120	
Sand	820	
Water	181	
Fiber (V_f)	0%, 0.25%, 0.5%	

Table 5- Mix proportion of concrete

Fiber dosage rates for 0.25% and 0.5% volume fractions were calculated to be 2.72 kg/m^3 and 5.5 kg/m^3 respectively.

3.3.2 Mortar mix design

To achieve equivalent concrete strength of mortar mix, cement/sand and water/cement design ratios were selected as 0.33 and 0.50 respectively. Same as concrete design mix, three types of mortar mix designs were formulated, as micro fibers were used in 3 different quantities. These mix designs were labelled as CMxx, 0.25%Mxx, and 0.5%Mxx, where CM refers to control mortar i.e. 0% fibers, percentage fraction in remaining two mix design indicate fiber volume fraction used in that mix design, M refers to mortar, and xx refers to sample identification number e.g. 0.25% M01 indicates

sample #1 for 0.25% mortar mix design. Moreover, fibers dosage rate was same as concrete as there was no change in fibers volume fraction. Mix proportion used for mortar is listed table 6.

Cement	736	Kg/m^3
Aggregate	0	
Sand	2207	
Water	368	
Fiber (Vf)	0%, 0.25%, 0.5%	

Table 6- Mix proportion of mortar

3.4 Mixing, Curing, & Setting Procedures

3.4.1 Concrete

ASTM C192 [23] has laid down the procedure for concrete mixing and curing. The first step in the mixing procedure was to weigh and batch ingredients as per required volume using a mix scale. For FRC, mixing procedure was started by first soaking fibers in ~20% of total water and holding for 15mins. This was done to change dry fibers into a slurry paste to promote uniform mixing with other ingredients. Once the slurry was formed, it was dumped into the drum mixer along with coarse aggregates and mixing was started for 2 mins. This was done as per manufacturer recommendation owing to the problem of conglomeration associated with micro cellulose fibers. Once the slurry was thoroughly mixed with coarse aggregates, remaining ingredients were added to the mixer and mixed for 3-mins followed by 3-mins rest time, and again a 2-min final mixing. For control concrete, the standard procedure outlined in ASTM C192 was followed.

Once the uniform blend was obtained and slump test performed, concrete was placed into molds. Molds were sprayed with WD40 chemical to provide ease in concrete removal once it is cured. Consolidation and compaction of concrete were obtained by placing

filled molds on a vibrating table for 30 secs; this was done to remove entrapped air from the mixture and to avoid honey comb structure.

Compacted concrete molds were placed at a room temperature for next 24hrs for initial curing and covered with a sheet of polyethylene to avoid water evaporation from the unhardened concrete. After the specified time was elapsed, hardened concrete samples were de-molded and placed in a water tub, which was maintained at 23.0 ± 2.0 ^{o}C for next 27 days for final curing.

3.4.2 Mortar

The sequence of steps followed for mortar mix was the same as the concrete mix. Ingredients were batched out as per required final volume of the mix using a weighing scale. However, with the absence of coarse aggregates, homogeneous blend of fibers in mortar mix was achieved by making fiber slurry and mixing it with sand for a minute in a bench mixer. Afterward, required cement and water quantities were added to the paste and blended for another two minutes. Once the uniform mix was achieved, the mortar was taken out of the bowl and placed into cube and briquette molds. Fig-8 shows filled cubes mold on left and filled briquette molds on right.

Figure 8 - Mortar mix in cube & briquette molds

To ensure maximum compaction and removal of entrapped air, poured mortar was manually tapped using a tapping rod. The mortar was placed in two equal layers in molds, and each layer was tapped 25 times. Once the molds were compacted, they were

covered and placed at room temperature for next 24hrs same as the concrete mix. Demolding was carried after 24hrs and samples were placed in a water tub maintained at 23.0 ± 2.0 ^{o}C for next 27 days for final curing.

3.5 Concrete testing

For concrete mixes, cylinders and beams were cast to determine the required parameters. The following testing procedures were employed for concrete testing.

3.5.1 Slump Test

Once uniform blend of the mix was obtained, slump test was carried out on all three design mixes to determine the workability of the mixes as per ASTM C143 [24]. A slump test is one of the test methods to indicate the workability of concrete, which is a measure of concrete's ability to be mixed, handled, placed, and consolidated with ease and minimal air entrapment [28].

Figure 9- Slump test of concrete design mixes; (L) CCxx, (R) 0.25% Cxx

3.5.2 Compressive strength

ASTM C39 [25] defines the procedure to determine the compressive strength of a concrete mix. 650K Lbs. Forney Test Pilot machine, shown in Fig 10-L, was used in this study. Five cylinders, having 4" diameter and 8" height each, were cast from all three-

concrete design mixes. To ensure smooth and flat surfaces of cylinders, they were first ground using the automated grinding machine shown in Fig 10-R.

Figure 10- (L) Compression test machine, (R) Grinding machine

Once ground, the cylinders were placed inside the machine one by one, then axial load was applied within the loading rate range prescribed by the standard until failure. As outlined in the standard, compressive strength for each cylinder was computed by dividing the peak load by the cross-section area of the cylinder. As five cylinders were tested for each design mix the average value for each mix was computed using below formula;

Compressive strength (MPa)= P/A

Where;

P = peak load (N)

A = cross section area (mm^2)

3.5.3 Flexural Strength

ASTM C1609 [26] defines the procedure to determine the flexural strength of a concrete beam. For this study, a closed loop testing system was employed using a servo controlled 250KN capacity MTS 810 testing machine. Beams were tested under four-point loading configuration to get the required load vs. deflection curve. Characteristic properties i.e.

flexural strength and toughness were computed using the data obtained from load vs. deflection curve.

ASTM C1609 recommends specimen sizes of 4” x 4” x 14”, and 6” x 6” x 20” for prismatic beams. Former dimensions were selected for prismatic beams in this study. However, test results generated using this standard is size dependent, and this fact needs to be accounted for when interpreting results of the same material with different specimen sizes.

Fig-11 depicts the four-point testing configuration. The distance between each roller was 4”, and a total span length of the beam was 12”. To get mid span deflection from the beam, a pair of Linear variable differential transformer (LVDT) was installed at the mid span with the help of deflection jig.

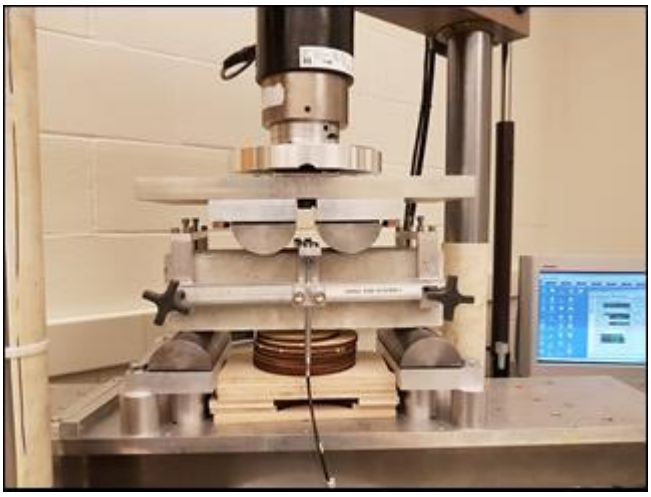

Figure 11- Four-point loading configuration

Before testing, LVDTs were calibrated using a lathe machine. Once calibrated, LVDT pair was attached to the jig and tests were conducted with a loading rate of 0.05mm/min in a deflection control closed loop mode. The sampling rate was set at 25Hz to get the maximum data points from each test. As specified in the standard, flexural performance of FRC at the first cracking is calculated by the first peak strength as was calculated using below formula;

Flexural Strength (MPa) = PL/bd^2

P = Load (N)

L = span length (mm)

B = specimen width (mm)

D = specimen depth (mm)

Also, above formula can be used to compute the flexural strength at any deflection.

3.6 Mortar testing

For mortar mixes, cubes and briquettes were cast to determine the required parameters. The following testing procedures were employed for mortar testing.

3.6.1 Compressive strength

ASTM C579 [27] states the method to determine the compressive strength of a mortar mix when tested in a cube shape. Six samples for each design mix were cast, and each had a dimension of 2” x 2” x 2”. Cubes were tested under a uniaxial compression testing machine, and peak load was measured at for each sample at the point of failure. Fig-12 shows fractured cube specimens after testing.

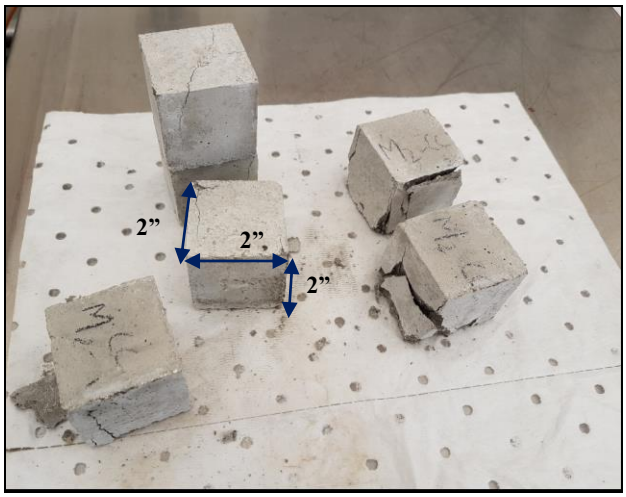

Figure 12 – Mortar cube specimens after compression testing

Loading rate was set within the standard’s specified range. As with compressive testing of concrete, compressive strength for each mortar specimen was computed using a formula;

Compressive strength (MPa) = P/A

P = Peak load (N)

A = cross section area (mm^2)

3.6.2 Tensile strength

ASTM C307 [28] defines the procedure to evaluate a mortar mix under uniaxial tension testing in the form of a dog-bone shape (briquette) sample having dimensions of 1” (depth) x 3” (length) x 1” (width at the center). Fig-13 shows the shape of briquette samples that were cast for the testing.

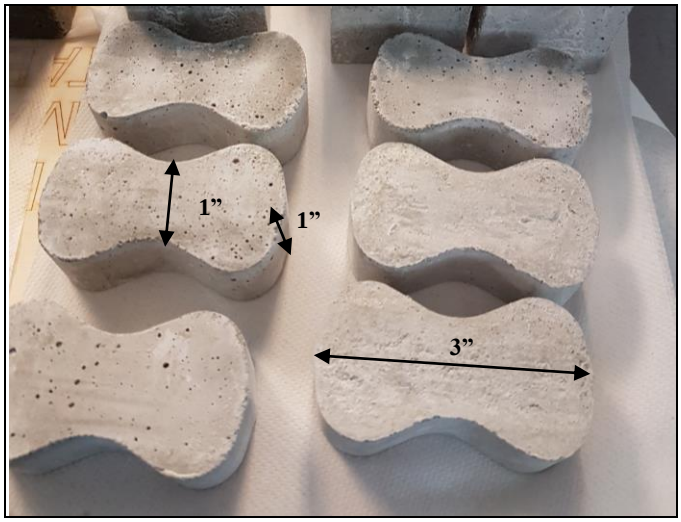

Figure 13 - Briquette samples

Six samples of each mortar design mix were tested using the test setup shown in Fig-14. Each specimen was clamped in a pair of bronze alloy grips which was attached to a testing frame having a load capacity of 7.1KN. Data was recorded at 25hz frequency, and three different crosshead displacement rates i.e. 2mm/min, 1.05mm/min, and 0.48mm/min were used. Different crosshead displacement rates were chosen to identify any potential post cracking strength response for each mortar design mix.

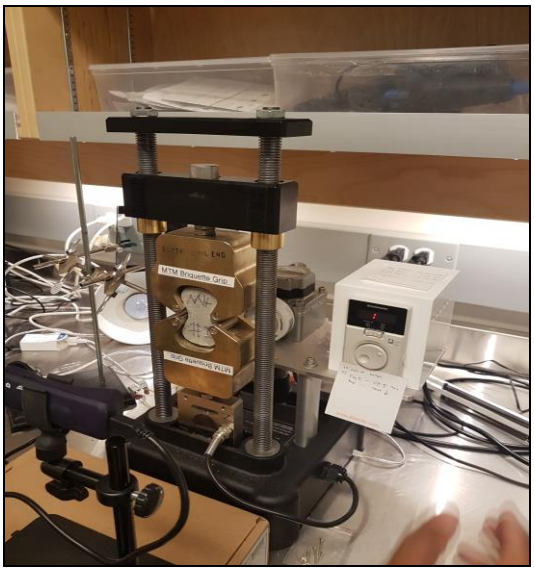

Figure 14 - UTM setup

The following formula was used to compute the uniaxial tensile strength of specimens;

Tensile strength (MPa) = P/ (b x d)

Where;

P = applied load (N)

B = Width at the center of briquette specimen (mm)

D = Depth at the center of briquette specimen (mm)

4 Results and Discussion

4.1 Concrete Results

The following section highlights the results obtained for concrete design mixes and discusses the effects of fiber addition on concrete properties.

4.1.1 Slump test

Table 7 depicts the associated slump with each mix;

Mix Design	Slump value	% diff. from CCxx
CCxx	30 mm	0%
0.25%Cxx	5 mm	-83.3%
0.5%Cxx	n/a	n/a

Table 7 - Slump test result of concrete design mixes

The decrease of 89% was observed in 0.25%Cxx slump value when compared to CCxx. This reduction in the slump is attributed to the loss of water in cement paste as cellulose fibers are hydrophilic and they tend to soak up most of the water during mixing. As the decrease in the slump value for 0.25%Cxx was considerable, slump test was not performed for 0.5%Cxx design mix as it was expected to be zero. The logic was based on the fact that fiber dosage rate in 0.5%Cxx mix was two times the 0.25%Cxx mix.

4.1.2 Compressive strength

The compressive strength of all three design mixes was measured at 28 days as per ASTM C39 [25] after wet curing. The following table shows the average compressive strength of each design mix after 28 days.

Mix Design	28 Days compressive strength (MPa)	
	Strength (MPa)	Average ± STDV
CCxx	35.5	35.4 ± 0.55
	35.4	
	34.5	
	36.2	
	35.2	
0.25%Cxx	37.9	37.6 ± 0.82
	36.8	
	36.5	
	38.8	
	38.0	
0.5%Cxx	37.3	37.8 ± 0.59
	38.4	
	37.4	
	38.6	
	37.1	

Table 8 - Compressive strength result of concrete design mixes

The above data was analyzed for % change in compressive strength in each design mix with an addition of cellulose fibers and is shown in a Fig-15.

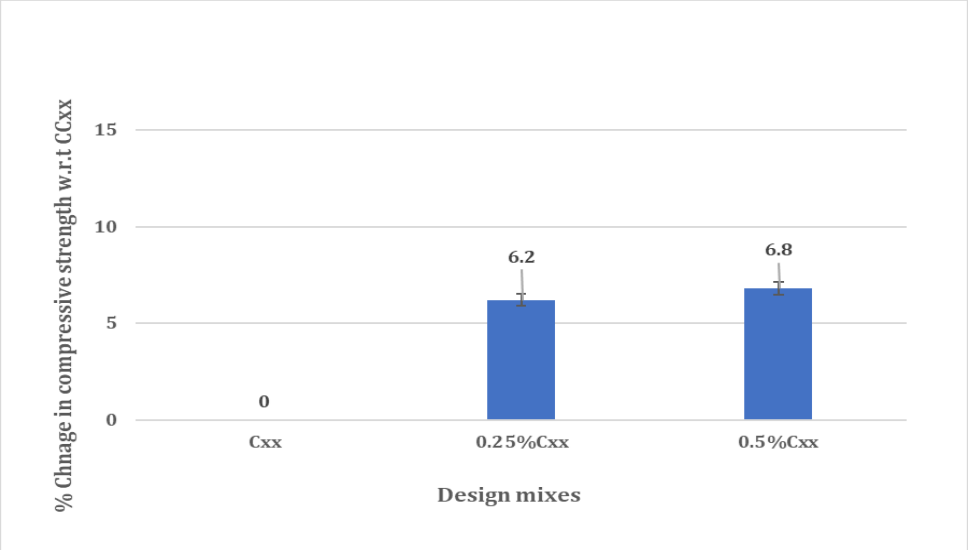

Figure 15 - Effect of fiber addition on concrete compressive strength

It is observed that minimal change i.e. 6.2% and 6.8% increase is noticed in the compressive strength of 0.25%Cxx and 0.5%Cxx design mixes, and this is in line with the general understanding of the effect of fiber addition on compressive strength of concrete.

Fiber presence mostly alters the failure mode of concrete by making them less brittle and slightly increases or decrease the compressive strength as compared to concrete without any fibers [29].

4.1.3 Flexural Strength

As it is shown in the literature review section, addition of fibers has a significant effect on flexural and toughness properties of the concrete. To check the effects of addition of cellulose fibers in concrete, the flexural test was carried out as described in the experimental section.

Table 9 shows the 28 days flexural strength, along with corresponding net deflection at the time of first cracking, of design mixes when tested in the form of prismatic beam under 4-point loading configuration;

Mix Design	28 Days Flexural strength - ASTM C1609			
	Strength (MPa)	**Avg. strength ± STDV**	**Deflection @ first crack (mm)**	**Avg. deflection ± STDV**
CCxx	6.08	5.88 ± 0.21	0.042	0.037 ± 0.003
	5.97		0.032	
	5.58		0.038	
0.25%Cxx	6.96	6.78 ± 0.19	0.056	0.053 ± 0.003
	6.59		0.050	
0.5%Cxx	5.94	5.93 ± 0.07	0.048	0.049 ± 0.004
	5.84		0.054	
	6.02		0.044	

Table 9 - Flexural strength data of concrete design mixes

Results for each design mix that deviated from more than 15% of mean value has been removed from the table. The above results have been analyzed in the form of percentage increase in flexural strength compared to control concrete and are shown Fig-16.

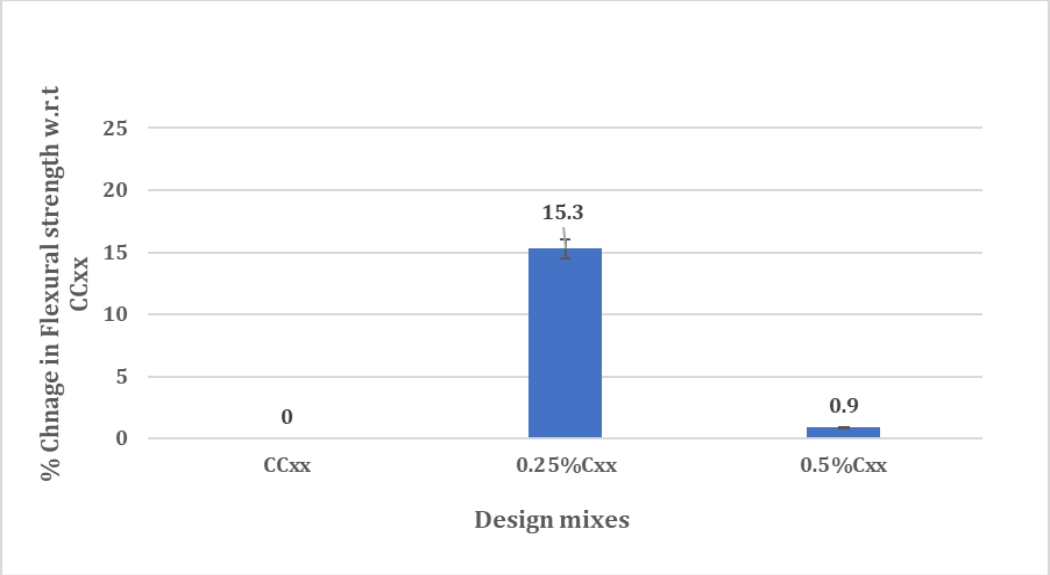

Figure 16 - Fibers effect on flexural strength of concrete design mixes

It is evident that a 0.25% volume fraction of fibers has a significant effect on the flexural properties of the concrete as compared to a 0.5% volume fraction of fibers in concrete. Along with the flexural strength increase of 15.3% for 0.25%Cxx, a considerable increase in its net deflection at first cracking is also noted. However, it is noted that fiber addition had no effect on post cracking strength of concrete.

Usually the addition of fibers increases the flexural strength of concrete, however in this study a significant drop in flexural strength of concrete is noted when fiber volume fraction was increased from 0.25% to 0.5%. The decrease in strength is because fibers fibrillation didn't take place effectively in 0.5%Cxx design mix, which in turn is attributed to hydrophilic nature of fibers and increase in surface areas of fibers that resulted in a dry design mix. This dry design mix was the cause of inadequate compaction of specimens and hence resulted in a significant drop in flexural strength of concrete when the fiber volume fraction increased from 0.25% to 0.5%.

4.1.4 Back calculation of tensile properties from flexural properties

Mobasher, et al. has proposed an inverse analysis approach to measure the tensile properties of FRC from flexural test result data [30] [31] [32]. As flexural tests are easy to perform and routinely conducted on FRCs' as a quality control measure, need to

correlate flexural response to reliable tensile properties has gained much attention of researchers. In this method, stress-strain models of FRCs are generated using experimental load deflection data using closed form equations.

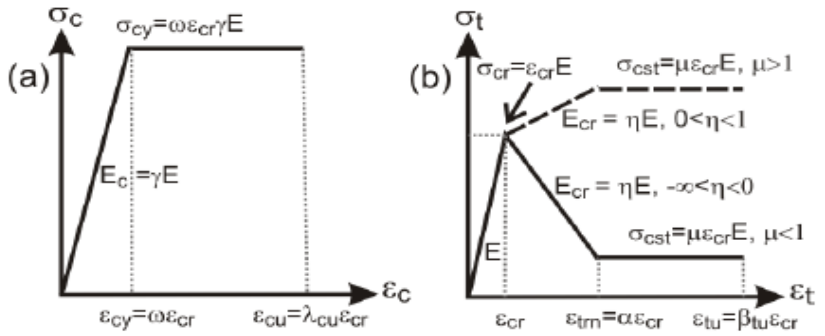

Figure 17 - Constitutive model for homogenized FRCs (L) compression model (R) Tension model [28]

As indicated in the Fig-17, the linear portion of an elastic perfectly plastic compression model terminates at ε_{cy} and σ_{cy}, which marks the end of the yield point. Elastic modulus for compression model is given by E_c. Stress level remains constant after reaching yield point, and the compression response terminates at strain ε_{cu}. Tension model, depicted in Fig 17, is described by a trilinear response. The first stage of elastic response is represented by E, second stage of post cracking behavior by E_{cr}, and third stage of constant stress by σ_{cst}. The same model can be used to represent strain hardening or strain softening response of FRC by changing E_{cr} value to either positive or negative. Tensile response terminates at ε_{tu} which is described as an ultimate tensile strain level. Constitutive stress-strain relationship for both models are expressed as follow [30] [31] [32];

$$\sigma_c(\varepsilon_c) = \begin{cases} E_c\varepsilon_c & 0 \le \varepsilon_c \le \varepsilon_{cy} \\ E_c\varepsilon_{cy} & \varepsilon_{cy} \le \varepsilon_c \le \varepsilon_{cu} \\ 0 & \varepsilon_c > \varepsilon_{cu} \end{cases}$$

$$\sigma_t(\varepsilon_t) = \begin{cases} E\varepsilon_t & 0 \le \varepsilon_t \le \varepsilon_{cr} \\ E\varepsilon_{cr} + E\varepsilon_t(\varepsilon_t - \varepsilon_{cr}) & \varepsilon_{cr} \le \varepsilon_t \le \varepsilon_{trn} \\ \mu E\varepsilon_{cr} & \varepsilon_{trn} \le \varepsilon_t \le \varepsilon_{tu} \\ 0 & \varepsilon_t > \varepsilon_{tu} \end{cases}$$

Where ε_c, ε_t, σ_c, and σ_t, represent compressive and tensile strains and stresses respectively. To obtain non-dimensional form of closed form solutions for moment curvature response, material parameters listed in Fig 1.1a & 1.1b are redefined in the form of seven parameters normalized with respect to intrinsic materials parameters E and ε_{cr}.

$$\omega = \frac{\varepsilon_{cy}}{\varepsilon_{cr}} \qquad \alpha = \frac{\varepsilon_{trn}}{\varepsilon_{cr}}$$

$$\beta_{tu} = \frac{\varepsilon_{tu}}{\varepsilon_{cr}} \qquad \lambda_{cu} = \frac{\varepsilon_{cu}}{\varepsilon_{cr}}$$

$$\gamma = \frac{E_c}{E} \qquad \mu = \frac{\sigma_{cst}}{E\varepsilon_{cr}}$$

$$\mu = \eta(\alpha - 1) + 1$$

As three parameter η, μ, and α are dependent on each other, these are only applicable to the tensile model if a response of FRC is considered up to the transition point. Similarly, normalized compressive strain, λ, at top fiber and normalized tensile strain, β, at bottom fiber are defined as

$$\beta = \frac{\varepsilon_{tbot}}{\varepsilon_{cr}} \qquad \lambda = \frac{\varepsilon_{ctop}}{\varepsilon_{cr}}$$

Relationship between both λ and β is defined by the normalized neutral axis parameter, K such as;

$$\frac{\lambda\varepsilon_{cr}}{kd} = \frac{\beta\varepsilon_{cr}}{d - kd}$$

Which can be further simplified as;

$$\frac{\lambda \varepsilon_{cr}}{kd} = \left(\frac{k}{1-k}\right)\beta$$

Now the constitutive stress-strain tension and compression models can be represented by above derived normalized parameters;

$$\frac{\sigma_c(\lambda)}{E\varepsilon_{cr}} = \begin{cases} \gamma\lambda & 0 \le \lambda \le \omega \\ \gamma\omega & \omega \le \lambda \le \lambda_{cu} \\ 0 & \lambda_{cu} < \lambda \end{cases}$$

$$\frac{\sigma_t(\beta)}{E\varepsilon_{cr}} = \begin{cases} \beta & 0 \le \beta \le 1 \\ 1 + \eta(\beta - 1) & 1 < \beta \le \alpha \\ \mu & \alpha < \beta \le \beta_{tu} \\ 0 & \beta_{tu} \le \beta \end{cases}$$

4.1.4.1 Moment Curvature relationship in term of normalized parameters

By ignoring shear deformation and assuming linear strain distribution in a rectangular cross section of beam having depth d and width b under flexural loading, stress-strain relationships presented in Fig 17 can be used to compute stress distribution across the cross section of beam at three stages of tensile strain i.e. $0 \le \beta \le 1$, $1 < \beta \le \alpha$, and $\alpha < \beta \le \beta tu$. For second and third stages, there are two possible scenarios i.e. λ can either be elastic ($0 < \lambda \le \omega$) or plastic ($\omega < \lambda < \lambda cu$).

For each stage, equilibrium of forces is used to compute the value of K (neutral axis depth ratio), which is followed by the computation of moment capacity found out by taking compression and tension forces around the neutral axis. Finally, corresponding curvature associated with moment is computed by dividing Ɛctop by neutral axis depth. Once the values of moment, M, and curvature, Ø, are obtained, they are normalized with respect to cracking moment, M_{cr}, and cracking curvature Øcr and represented as M` and Ø`.

The following equations along with equations listed in the table are used to compute neutral axis value and moment curvature for all stages of applied strain [30] [31] [32];

$$M(\lambda, k, \omega, \mu) = M_{cr} M`(\lambda, k, \omega, \mu)$$

$$M_{cr} = \frac{1}{6} b d^2 E \varepsilon_{cr}$$

$$\phi(\lambda, k, \omega, \mu) = \phi_{cr} \phi`(\lambda, k, \omega, \mu)$$

$$\phi_{cr} = \frac{2\varepsilon_{cr}}{d}$$

Stage	Parameters	K	$M_i` = \frac{M}{M_{cr}}$	$\phi_i` = \frac{\phi}{\phi_{cr}}$
1	$0 < \beta \leq 1$	$K_1 = \begin{cases} \frac{1}{2} & for\ \gamma = 1 \\ \frac{-1+\sqrt{\gamma}}{-1+\gamma} & for\ \gamma \neq 1 \end{cases}$	$M_1` = \frac{2\beta[(\gamma-1)K_1^3 + 3K_1^2 - 3K_1 + 1]}{1 - K_1}$	$\phi_1` = \frac{\beta}{2(1-K_1)}$
2.1	$0 < \beta \leq \alpha$ $0 < \lambda \leq \omega$	$K_{21} = \frac{D_{21} - \sqrt{D_{21}\gamma\beta^2}}{D_{21} - \gamma\beta^2}$ $D_{21} = \eta(\beta^2 - 2\beta + 1) + 2\beta - 1$	$M_{21}` = \frac{(2\beta^3 - C_{21})K_{21}^3 + 3C_{21}K_{21}^2 - 3C_{21}K_{21} + C_{21}}{1 - K_{21}}$ $C_{21} = \frac{(2\beta^3 - 3\beta^2 + 1)\eta + 3\beta^2 - 1}{\beta^2}$	$\phi_{21}` = \frac{\beta}{2(1-K_{21})}$
2.2	$0 < \beta \leq \alpha$ $\omega < \lambda \leq \lambda_{cu}$	$K_{22} = \frac{D_{22}}{D_{22} + 2\omega\gamma\beta}$ $D_{22} = D_{21} + \gamma\omega^2$	$M_{22}` = (3\gamma\omega\beta^2 + C_{22})K_{22}^2 - 2C_{22}K_{22} + C_{22}$ $C_{22} = C_{21} - \frac{\gamma\omega^3}{\beta^2}$	$\phi_{22}` = \frac{\beta}{2(1-K_{22})}$
3.1	$\alpha < \beta \leq \beta_{tu}$ $0 < \lambda < \omega$	$K_{31} = \frac{D_{31} - \sqrt{D_{31}\gamma\beta^2}}{D_{31} - \gamma\beta^2}$ $D_{31} = \eta(\alpha^2 - 2\alpha + 1) + 2\mu(\beta - \alpha) + 2\alpha - 1$	$M_{31}` = \frac{(2\gamma\beta^3 - C_{31})K_{31}^3 + 3C_{31}K_{31}^2 - 3C_{31}K_{31} + C_{31}}{1 - K_{31}}$ $C_{31} = \frac{(2\alpha^3 - 3\alpha^2 + 1)\eta - 3\mu(\alpha^2 - \beta^2) + 3\alpha^2 - 1}{\beta^2}$	$\phi_{31}` = \frac{\beta}{2(1-K_{31})}$
3.2	$\alpha < \beta \leq \beta_{tu}$ $\omega < \lambda \leq \lambda_{cu}$	$K_{32} = \frac{D_{32}}{D_{32} + 2\omega\gamma\beta}$ $D_{32} = D_{31} + \gamma\omega^2$	$M_{32}` = (3\gamma\omega\beta^2 + C_{32})K_{32}^2 - 2C_{32}K_{32} + C_{32}$ $C_{32} = C_{31} - \frac{\gamma\omega^3}{\beta^2}$	$\phi_{32}` = \frac{\beta}{2(1-K_{32})}$

Table 10 - Expressions for normalized parameters K, M`, and Ø`[30] [31] [32]

To generate a moment curvature diagram for a given set of parameters and beam dimension, value of λ can be substituted incrementally from zero to failure that result into either deflection hardening (μ < μcrit) or deflection softening (μ > μcrit) response of moment curvature. Here μcrit is defined as

$$\mu_{crit} = \frac{\omega}{3\omega - 1}$$

4.1.4.2 Computation of Load Deflection Response

The load deflection response of a beam can be derived using moment curvature response, moment area method, and crack localization rules as described below [31];

1. For a given beam, moment curvature response is generated using moment curvature equations described in the previous section where value of β is incrementally imposed. For stage 2 and 3 against each value of β, λ (compressive strain) condition is verified either as λ < ω or λ > ω.

2. The maximum allowed load on beam's cross section is determined by the moment curvature diagram, and applied load vectors P=2M/S is computed using discrete moments along the diagram where S is the spacing between supports.

3. The beam is segmented into finite sections, and for a given load, static equilibrium condition is employed to compute moment distribution along the beam and crack localization rules along with moment curvature relationship to identify curvature.

4. Mid-span deflection is computed by moment area method of curvatures between mid-span and support. This procedure is employed at each step load until complete load deflection response is computed.

The following equation is used to calculate the maximum deflection at mid-point at the time of first cracking and during four-point bend test [30] [31] [32];

$$\delta_{cr} = \frac{23}{216} L^2 \phi_{cr}$$

Similarly, below equations are used to compute the post crack maximum deflection at mid-span of the beam for four-point bend test

$$\delta_u = \frac{L^2}{216M_u^2}\{(23M_u^2 - 4M_uM_{cr} - M_{cr}^2)\phi_u + (4M_u^2 + 4M_uM_{cr})\phi_{cr}\} \qquad \mu > \mu_{crit}$$

$$\delta_u = \frac{5\phi_u L^2}{72} + \frac{M_u L^2 \phi_{cr}}{27M_{cr}} \quad \mu < \mu_{crit}$$

As discussed above that closed form equations can be used to generate a tensile response of material from its flexural test data. In this section, the procedure used to generate a tensile response of all three concrete mix designs for their experimental flexural test results has been discussed. However, only one mix design i.e. 0.5%C01 is shown as an example here while data for rest of the design mixes has been attached in the appendix [DI – DIII].

The algorithm developed by Mobasher et al. [33] has been used to generate the response by first generating a simulated load vs. deflection response of the material and matching it with the experimental load vs. deflection data of the beam. To do so, the following sequence of input data was used to generate the simulated load vs. deflection response;

1. Beam dimensions i.e. Length, width, and depth
2. Loading configuration i.e. 3-point or 4-point
3. Elastic modulus of concrete, E. This value was generated based on trial and error such that elastic portion of simulated curve matched with elastic portion of experimental curve
4. Ɛcr value also selected by trial and error to match the peak at cracking
5. Parameters α, μ, and η are dependent on each other such that one among them is determined by other 2. Parameter α effects the horizontal location of a transition point, parameter μ adjust the vertical position of a transition point, and parameter η changes the post cracking slope. Values for all three parameters were selected by trial and error method.

Moment Curvature & Load Deflection Response of Concrete Design Mix – 0.5%C01

The following values of input parameters were used to generate the response;

E	30000
ε_{cr}	0.00015
α	1.4
γ	0.9
η	-0.875
μ	0.65
b_{tu}	2.5
ω	9.35
λ_{cu}	40
μ_{crit}	0.97367

Table 11 - Input parameters for back calculation

By using the equations stated in previous sections and analysis procedures mentioned above, moment curvature response of 0.5%C01 mix was generated and is presented Fig-18

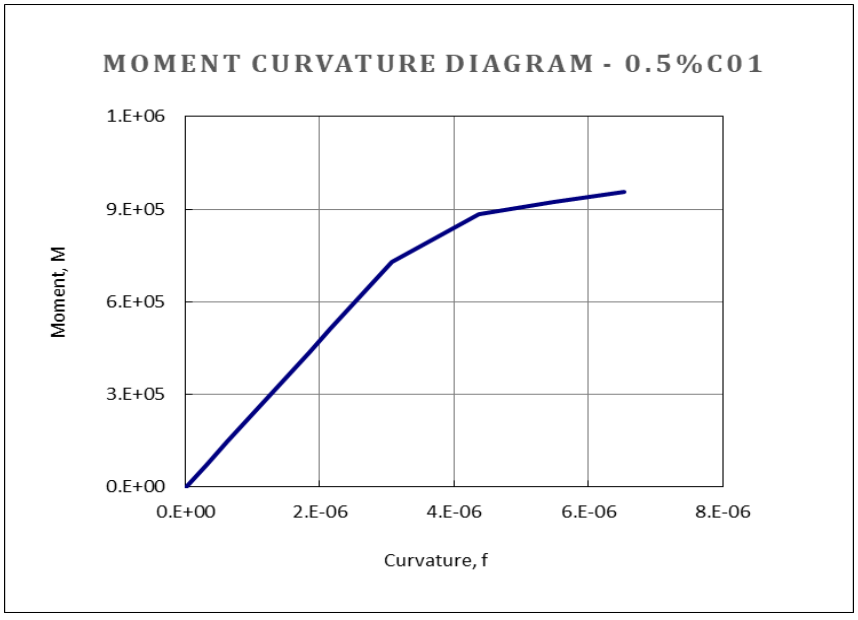

Figure 18 - Moment curvature response

Similarly, load vs. deflection response of the material was generated from moment curvature response, moment areas method, and crack localization rules as mentioned in the literature review section;

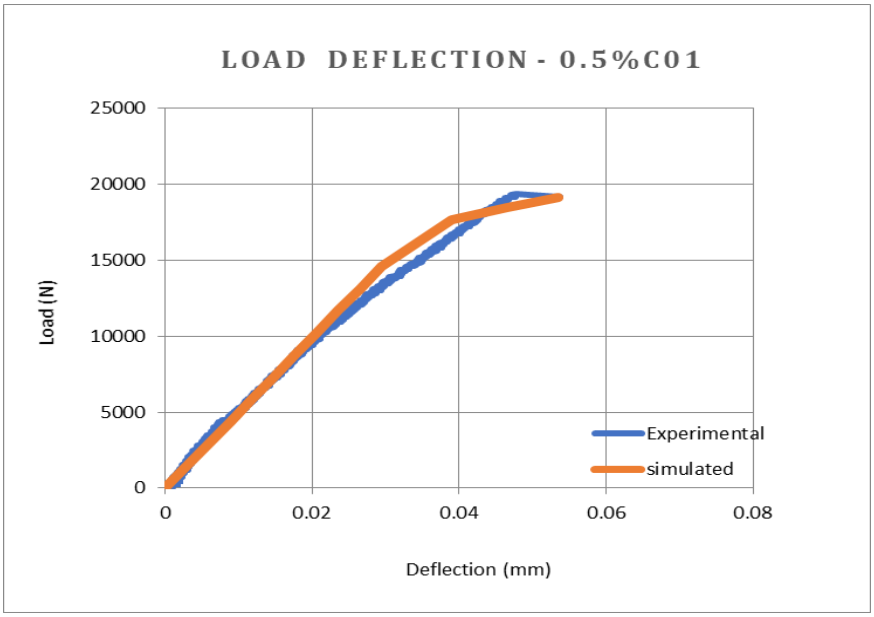

Figure 19 - Experimental and simulated load vs deflection response

Simulated load (modelled load) vs. deflection response matched very well with experimental load vs. deflection response. Also, no post cracking strength was observed as material broke in a brittle fashion.

Tensile and Compressive response of 0.5%C01

Tensile and compressive responses of the material at different stages were determined by the normalized equations used to describe trilinear tension and bilinear compression models of the materials as shown in the following Fig 20-21.

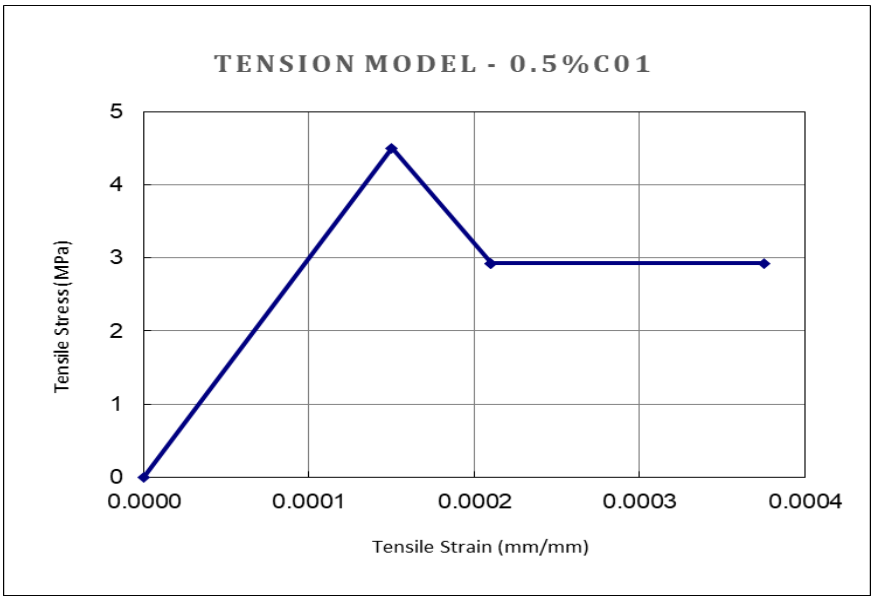

Figure 20 - Back calculated tension model - 0.5%C 01

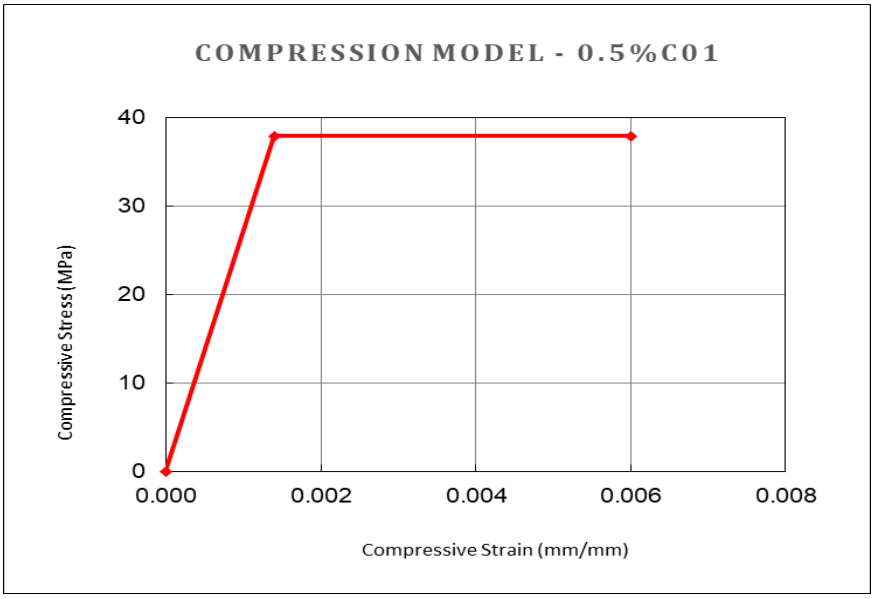

Figure 21 - Back calculated compression model - 0.5%C 01

Tensile and compressive normalized parameters deducted from above graphs are listed in Table 12.

Tension Model Parameters					
Strain			Stress		
Parameters		Units	Parameters		Units
ε_{cr}	0.00015	(mm/mm)	σ_{cr}	4.5	(MPa)
ε_{trn}	0.00021		σ_{trn}	2.925	
ε_{trn}	0.00021		σ_{cst}	2.925	
ε_{tu}	0.000375		σ_{tu}	2.925	

Table 12 - Back calculated parameters for tension and compression model

4.1.4.3 Tensile response of concrete design mixes

As described in the above section, the same procedure was followed for each concrete design mix, and corresponding tensile and compressive models were generated. In all three design mixes, no post cracking ductile behavior was observed, and all of them failed in a brittle manner after the generation of the first crack. Average tensile strain parameter for all three concrete design mixes is shown in Table 13.

Design Mix	Stress parameters (MPa)			Strain parameters (mm/mm)		
	Average values					
	σ_{cr}	σ_{trn}	σ_{tu}	ε_{cr}	ε_{trn}	ε_{tu}
CCxx	3.88	2.58	2.58	0.00009	0.00020	0.00036
0.25%Cxx	5.04	3.03	3.03	0.00018	0.00037	0.00050
0.5%Cxx	4.25	2.89	2.89	0.00013	0.00019	0.00040

Table 13 - Average back calculated parameters for tension model of concrete design mixes

The above data was analyzed for % change in back calculated tensile strength in each design mix with an addition of cellulose fibers and is shown in Fig -22.

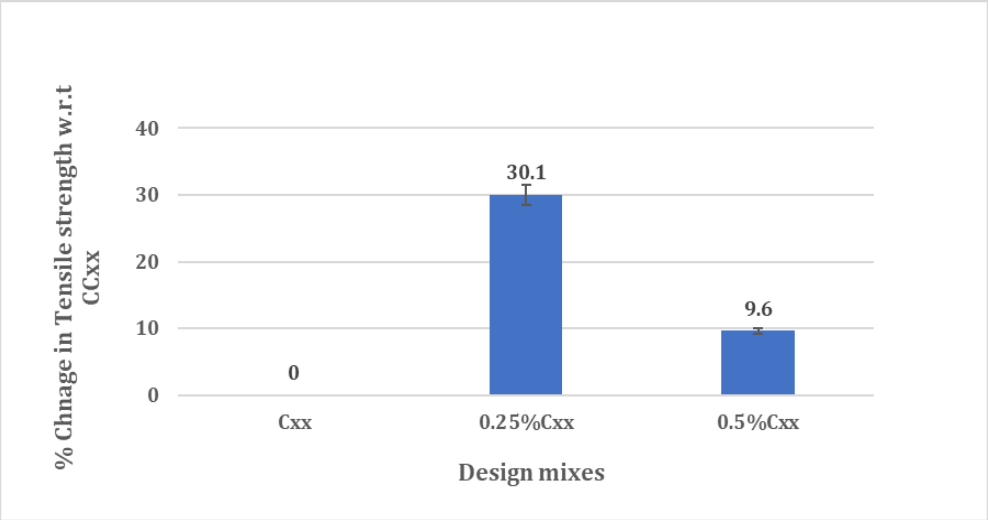

Figure 22 - Effect of fibers addition on Back Calculated Tensile Strength of concrete

It is evident from the above graph that the 0.25% fiber volume fraction had the most significant effect on tensile properties of concrete. The result presented here matches well with the flexural strength of concrete design mixes where 0.25%Cxx had shown a significant increase in flexural strength.

4.2 Mortar Results

This section elaborates the results obtained for mortar design mixes and discusses the fiber addition effects on mortar mix design

4.2.1 Compressive strength

28 days compressive strength of all three design mixes, in the form of cube specimens, was measured at as per ASTM C579 [27] after wet curing. The following table shows the average compressive strength of each design mix after 28 days.

Mix Design	28 Days compressive strength (MPa)	
	Individual	**Average ± STDV**
CMxx	38.96	43.87 ± 2.32
	44.20	
	47.23	
	43.01	
	43.50	
0.25%Mxx	52.84	48.76 ± 3.09
	50.65	
	48.30	
	43.10	
	47.25	
	50.40	
0.5%Mxx	56.76	53.55 ± 2.28
	55.68	
	52.88	
	52.68	
	49.64	
	53.68	

Table 14 - Compressive strength result of mortar design mixes

Results for each design mix that deviated from more than 15% of the mean value have been removed from the table. The above data was analyzed for % change in compressive strength in each design mix with an addition of cellulose fibers and is shown in Fig-23.

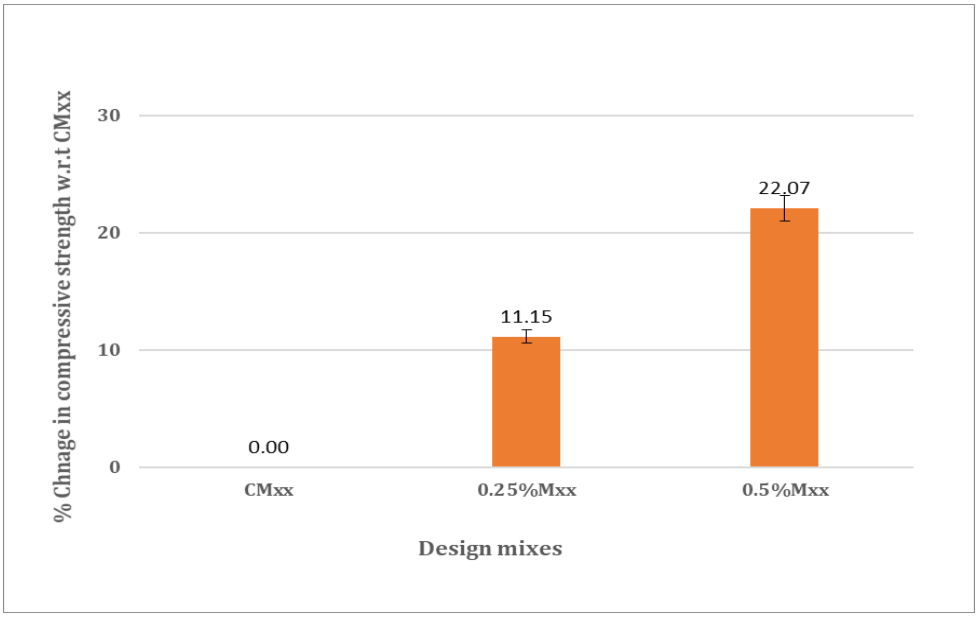

Figure 23 - Effect of fiber addition on mortar compressive strength

A considerable increase in compressive strength of mortar is noticed with an increase in fiber volume fraction from 0% to 0.5%. This increase in compressive strength is attributed to the internal curing, which itself is reflected in the performance characteristics of cellulose fibers provided by the manufacturer [22]. As the name suggests, internal curing is a method of providing additional water for improved hydration using pre-wetted pockets of fibers or aggregates that release water when required for improved hydration. For both mortar and concrete mix designs, fibers were pre-wetted by being soaked in the water before adding them to the mixer. Increase in compressive strength for mortar is significant when compared to concrete mix designs, and this can be understood in the light of mix design used for both concrete and mortar. As mortar had more cement content (736Kg) available per m^3 as compared to concrete (where cement content was 340 Kg/m^3), this could have led to an overall increase in the hydration process in the mortar which was further improved by the internal curing.

4.2.2 Uniaxial tensile testing

28 days uniaxial tensile strength of all three design mixes, in the form of briquette specimens, was measured at as per ASTM C307 [28]. Also, to identify any post cracking strength response of mortar mix designs, different values of machine crosshead displacement rates were used. Table 15 shows the results of testing.

Mix Design		Ultimate Tensile Strength (MPa)			Average ± STDV
		Displacement rate			
		2mm/min	1.05mm/min	0.48mm/min	
CMxx	CM 01	4.33	-	-	4.2 ± 0.21
	CM 02	4.39			
	CM 03	4.38			
	CM 04	-	4.32		
	CM 05		3.85		
	CM 06		3.95		
0.25%Mxx	0.25% M01	-	4.12	-	4.16 ± 0.42
	0.25% M03		4.49		
	0.25% M04		-	4.36	
	0.25% M05			4.05	
	0.25% M06			3.82	
0.5%Mxx	0.5% M01	-	3.78	-	3.53 ± 0.23
	0.5% M02		3.15		
	0.5% M03		3.30		
	0.5% M04		-	3.60	
	0.5% M05			3.71	
	0.5% M06			3.67	

Table 15 - Tensile strength result of mortar design mixes

Displacement rates mentioned above are not from the samples, rather they represent the machine crosshead displacement rate. Ideally, a graph between tensile strength and sample displacement (using LVDT) is generated in the above experiment, however owing

to limitations it was assumed that if samples are held tightly in the grips without any slippage, machine crosshead displacement rate can be regarded as a representative sample displacement rate.

Graphical representation of above results has been attached in the appendix [B] which shows no post crack strength. It is evident from the above results that displacement rate had no significant effect on the ultimate tensile strength of mortar mix designs hence average strength value for each mix design can be used as a reference value for data analysis.

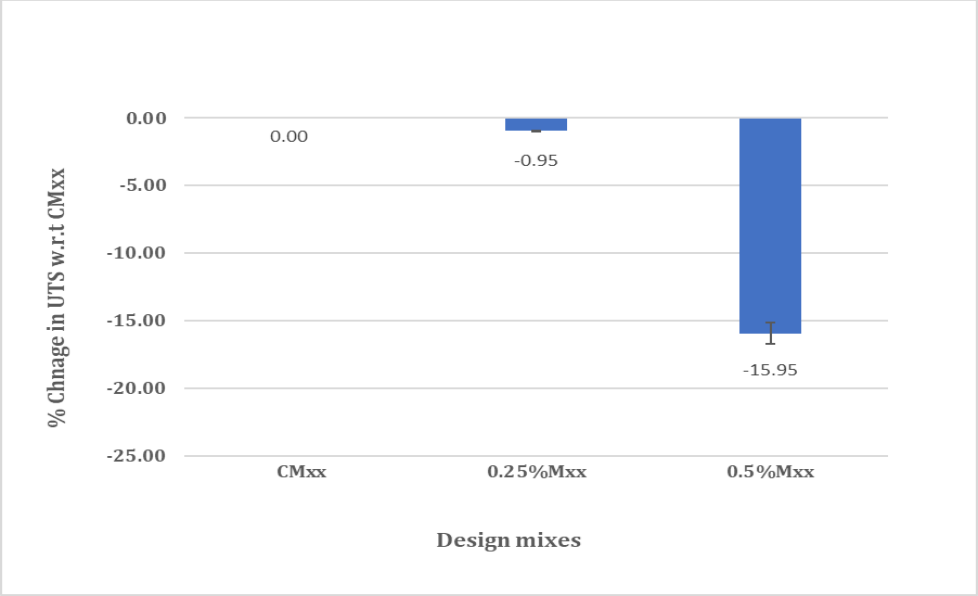

Figure 24 - Effect of fiber addition on ultimate tensile strength (UTS) of mortar mix designs

With an increase in fiber volume fraction from 0% to 0.5%, a significant decrease in UTS of mortar mix design is observed. The decrease could have happened due to poor dense structure which was due to the dry nature of mortar mix designs as fiber volume fraction was increased. Also, as hand tapping was used to compact the samples, considerable chances exist that variation in process and poor compaction led to the generation of pore network inside samples, and this was compounded by the presence of un-fibrillated fiber pockets as volume fraction was increased from 0.25% to 0.5%. This claim was supported by the visual analysis of both mix designs fractured surfaces in which 0.5%Mxx showed

the presence of un-fibrillated fibers pockets and a pore network as compared to 0.25%Mxx as seen in Fig-25.

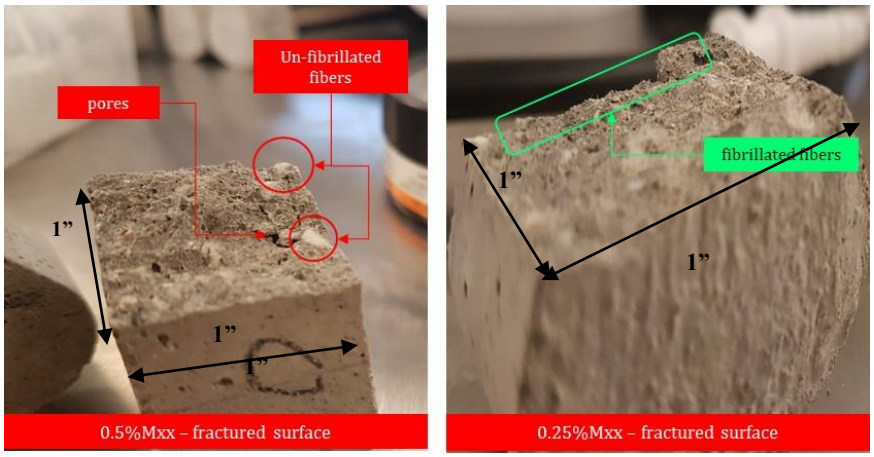

Figure 25 - Fractured surfaces close-up (L) 0.5% Mxx (R) 0.25% Mxx

4.3 Analysis of tensile strength from Uniaxial tension testing data and Back calculation procedure

Tensile strength computed through indirect and direct method is shown Fig-26.

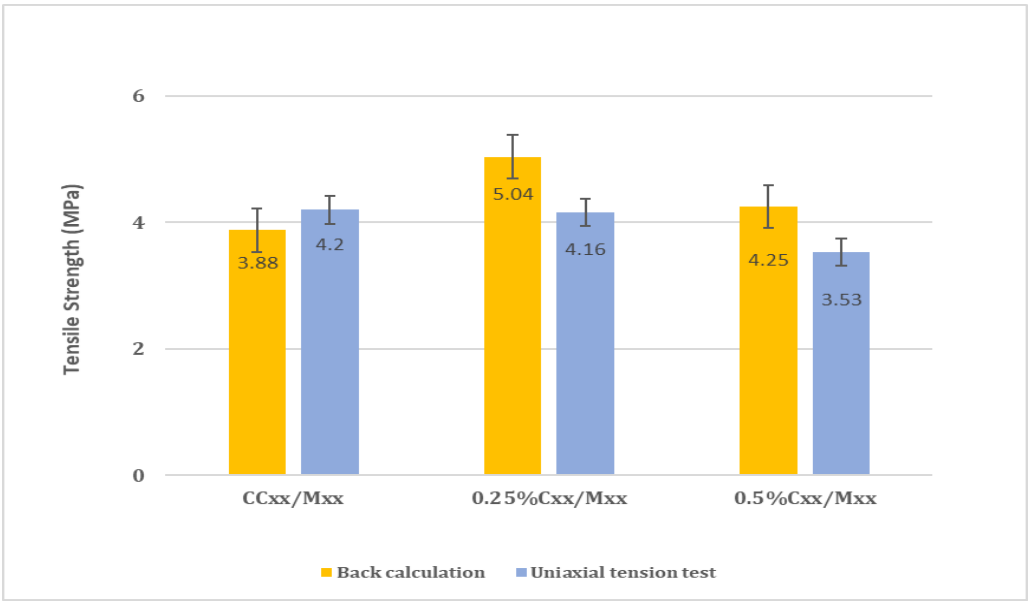

Figure 26 - Comparison of Tensile strengths computed by tension and flexural tests

If underlying assumption was valid, tensile strength computed through both methods should have been in close agreement. However, as mortar and concrete are two different types of materials, both tend to have a different response when subjected to tensile stresses. The difference in response is due to presence of coarse aggregates in concrete that alter its behavior.

5 Conclusion

Below are the main observations based on the experimental study employed in this project;

1. Micro cellulose fibers are hydrophilic and caused a decrease in the workability of concrete. This was noted during the experimental work, where slump value had shown a major decrease of ~89% as soon as fibers were added to the design mix. It is recommended to incorporate a relevant admixture in the mix design to improve the workability of concrete.

2. Micro cellulose fibers addition didn't show any significant effect on the compressive strength of concrete. In fact, a maximum of 6.8% increase in compressive strength was noted in the 0.5%Cxx mix design. This finding is in line with the general understanding of fiber effects on concrete compressive strength.

3. Micro cellulose fibers addition had shown no effect on post cracking strength of concrete as specimens of all three mix designs fractured in a brittle manner after reaching a maximum load. However, with the fibers addition concrete had shown an increase in maximum load capacity hence effect on flexural strength was noticeable especially in 0.25%Cxx where a ~15% increase in strength was noted. With an increase in fiber volume fraction from 0.25% to 0.5%, flexural strength was decreased to a level of control concrete. This decrease was linked to the fibers inability to fibrillate thoroughly with an increase in volume fraction during mixing. This highlights the importance of optimum fiber dosage rate concerning a design mix.

4. The fiber dosage rates used in this study were 2.72 Kg/m^3 and 5.5 Kg/m^3. However, the manufacturer recommended dosage rate is ~ 1 Kg/m^3. A significant drop in flexural strength in 0.5%Cxx is attributed to increased dosage rate that had

rendered the fibers to fibrillate properly throughout the mixture ultimately causing a detrimental effect on concrete's properties regarding the fibers addition.

5. The compressive strength of mortar cubes had shown an increase in compressive strength with increasing fiber volume fraction. This increase is linked to the concept of internal curing, which is more prominent in mortar as compared to concrete. Cement volume fraction in mortar is almost double than the concrete, hence raising the possibility of an increase in the hydration process consequently increasing in compressive strength of mortar mix designs.

6. Results of uniaxial tension testing of mortar support the conclusion mentioned above regarding optimum fiber dosage rate. The overall decrease in ultimate tensile strength was noted with an increase in the fiber volume fraction as mixes became dry and fibers were unable to fibrillate thoroughly.

7. Ideally, ultimate tensile strength calculated from uniaxial tension test and back calculated from the flexural test for a given design mix should be in close agreement. However, this is not the case here.

    a. The underlying assumption made for mortar design mix was that absence of coarse aggregates has no/little effects on tensile properties when subjected to uniaxial tension test. However, concrete and mortar are two different materials, and the absence of coarse aggregates from mortar significantly effects its tensile behavior.

8. Overall, it has been concluded that micro cellulose fiber addition in concrete has a nominal effect on the mechanical properties of concrete, and these fibers don't contribute to residual load carrying capacity of the concrete hence causing it to fail in a brittle manner once peak load is reached. Mostly, micro cellulose fibers are used as a secondary reinforcement [19]. Also, this can also be understood from the perspective of critical fiber length (Lc) which is required to continue carrying the load once the matrix is cracked and the load is transferred to fibers. If fibers fall short of a critical length, they will be unable to continue carrying the load causing material failure [16].

9. The above conclusion is also supported by the fact that micro fibers addition mostly contributes to the durability aspect of concrete i.e. reducing plastic shrinkage cracking, reducing concrete permeability and absorption, etc. These fibers must be used in conjunction with appropriate macro fibers i.e. in a hybrid mode if the increase in residual load carrying capacity is required [16].

5.1 Future Work

This work can be further extended to include the following aspects;

1. The designing of a test fixture to test concrete in a tension mode as per recommendations laid down in RILEM TC 187-SOC [34], and comparing concrete's back calculated tension properties with it.

2. Performing Flexural test on notched specimens and using crack mouth opening displacement as a controlled mode.

3. Using micro cellulose fibers in conjunction with macro fibers to see the overall improvement in concrete durability and mechanical properties.

4. Performing fiber dispersion analysis of the fractured surfaces of beams and briquettes using SEM to better understand the ability of the micro cellulose fibers to fibrillate in a chosen concrete and mortar design mix.

5. Performing fracture toughness tests on micro cellulose fiber reinforced concrete to determine the a_c, K_{1c}, G_f, and CTOD as per RILEM test [35]. In this regard, study carried out by Sarah et al. showed the effects of micro cellulose fiber addition on critical crack length of RP concrete, it was noted that fibers addition didn't have any noticeable impact on the a_c value i.e. it changed from 0.019 m to 0.02 m [36].

6. Using a recommended fiber dosage rate of micro cellulose fibers as mentioned by the manufacturer.

6 Bibliography

1. World Commission on Environment and Development (WCED), Our common future: the brundtland report on environment and development, Oxford University Press, Oxford, 1987.

2. Banthia, et al. “Plant-based natural fibers reinforced cement composites: A review.” Cement and Concrete Composites, vol. 68, Feb. 2016, pp. 96–108.

3. ACI 116R-00: Cement and Concrete Terminology (Reapproved 2005).

4. ACI 544.1R-96: Fiber reinforced concrete (1999)

5. Nguyen Van CHANH, Steel Fiber Reinforced Concrete, Faculty of Civil Engineering, Ho Chi Minh City University of Technology.

6. Gopalaratnam, and S.P. Shah. "Failure Mechanisms and Fracture of Fiber Reinforced Concrete." American Concrete Institute, 1987.

7. Bentur, A., and S. Mindess. Fibre Reinforced Cementitious Composites. 2nd. New York, NY: Taylor & Francis, 2007.

8. He Tian, Y. X. Zhang, Chunhui Yang, Yining Ding. (2016) Recent advances in experimental studies of the mechanical behaviour of natural fibre-reinforced cementitious composites. Structural Concrete 17:4, pages 564-575.

9. Arsene, M. A., Okwo, A., Bilba, K., Soboyejo, A. B. O., Soboyejo, W. O.: Chemically and thermally treated vegetable fibers for reinforcement of cement-based composites. Materials and Manufacturing Processes, 2007, 22, pp. 214–227

10. John, V. M., Cincotto, M., Sjotrom, C., Agopyan, V., Oliveira, C. T. A.: Durability of slag mortar reinforced with coconut fibre. Cement and Concrete Composites, 2005, 27, pp. 565–574.

11. John, M. J., Anandjiwala, R. D.: Recent development in chemical modification and characterization of natural fiber-reinforced composites. Polymer Composites, 2008, 29, pp. 187–207.

12. R.S.P. Coutts, P. Kightly, Bonding in wood fibre cement composites, J. Mater Sci. 19 (1984) 3355 - 3359.

13. N. El-Ashkar, H. Nanko, K. Kurtis, Effect of Moisture State on Mechanical Behavior and Microstructure of Pulp Fiber-Cement Mortars, J. Mater Civ. Eng.19 (8) (2007) 691 - 699.

14. Shah, et al. “Fiber-matrix interaction in microfiber-reinforced mortar.” Advanced Cement Based Materials, vol. 2, March. 1995, pp. 53-61.

15. N. Banthia, R. Gupta, Hybrid fiber reinforced concrete (HyFRC): fiber synergy in high strength matrices, Mater. Struct. 37 (10) (2004) 707–716.

16. Banthia, et al. “Fiber synergy in Hybrid Fiber Reinforced Concrete (HyFRC) in flexure and direct shear.” Cement and Concrete Composites, vol. 48, Apr. 2014, pp. 91–97.

17. R. Gupta and N.Banthia, “Correlating plastic shrinkage cracking potential of fiber reinforced cement composites with its early-age constitutive response in tension”, Mater. Struct., no. 49, pp. 1499 – 1509, 2016.

18. ASTM C150 “Standard specification for Portland cement".

19. “UltraFiber Technical Bulletin UFTB#1, Plastic Shrinkage Crack Reduction.” ultrafiber500, Google, drive.google.com/file/d/0ByWupltkC24Lc2hvWTNMVWVoc3M/view?usp=sharing. Accessed 12 Aug. 2017.

20. “UltraFiber Technical Bulletin UFTB#2, Finishability.” ultrafiber500, Google, drive.google.com/file/d/0ByWupltkC24LS1VYRTV1ZmstR3c/view. Accessed 12 Aug. 2017.

21. “UltraFiber Technical Bulletin UFTB#7, Freeze/Thaw Durability.” ultrafiber500, Google, drive.google.com/file/d/0ByWupltkC24LRkltZlV2OXQzZGs/view. Accessed 12 Aug. 2017.

22. “UltraFiber 500 Product Information.” ultrafiber500, Google, drive.google.com/file/d/0ByWupltkC24LclBRQk5NcVJ6Ync/view. Accessed 12 Aug. 2017.

23. ASTM C192 “Standard practice for making and curing concrete test specimens in the laboratory”.

24. ASTM C143 “Standard test method for slump of hydraulic-cement concrete”.

25. ASTM C39 “Standard test method for compressive strength of cylindrical concrete specimens”.

26. ASTM C1609 “Standard test method for flexural performance of fiber reinforced concrete using third-point loading”.

27. ASTM C579” Standard test method for compressive strength of chemical-resistant mortars, grouts, monolithic surfacings, and polymer Concretes”.

28. ASTM C307” Standard test method for tensile strength of chemical-resistant mortar, grouts, and Monolithic Surfacing".

29. ACI 544.2R-89 Measurement of properties of fiber reinforced concrete (Reapproved 2009).

30. B. Mobasher, M. Bakhshi, and C. Barsby, “Back calculation of residual tensile strength of regular and high performance fiber reinforced concrete from flexural tests," vol. 70, pp. 243 -253, 2014.

31. B. Mobasher, “Closed-Form Moment-Curvature Expressions for Homogenized Fiber-Reinforced Concrete," no. 104, 2008.

32. C. Soranakom and B. Mobasher, “Flexural Modelling of Strain Softening and Strain Hardening Fiber Reinforced Concrete," High Perform. Fiber Reinf. Cem. Compos., vol. 5, pp. 155 - 164, 2007.

33. Mobasher, Barzin, and Yiming Yao. “A Spreadsheet-Based Inverse Analysis Procedure for Flexural Specimens – Strain Softening/Hardening Behavior.” 2015

34. Final report of RILEM TC 187-SOC “Experimental determination of the stress-crack opening curve for concrete in tension”.

35. RILEM Committee 50-FMC. Determination of the Fracture Energy of Mortar and Concrete by Means of Three-Point Bend Tests on Notched Beams. Materials and Structures, Vol. 18, No. 4, 1985, pp. 285–290.

36. Peters, J.S., Rushing, T.S., Landis, E.N., Cummins, T.K., 2010. Nanocellulose and Microcellulose Fibres for Concrete. Transportation Research Record: Journal of the Transportation Research Board, vol. 2, page 25-28

7 Appendices – A, B, C, & D

- Appendix A – Analysis reports of fine and coarse aggregates
- Appendix B – Concrete and mortar mix design calculations
- Appendix C – Uniaxial tension testing graphs
- Appendix D – Back calculation parameters, moment curvature response, tensile and compressive responses of all three concrete mix design specimens

Appendix: A-I (Aggregates sieve analysis report)

Golder Associates

SIEVE ANALYSIS OF FINE AND COARSE AGGREGATE

CSA A23.2-2A

LEHIGH MATERIALS, DIVISION OF LEHIGH HANSON MATERIALS LTD.
P.O. Box 1790
Sechelt, BC
V0N 3A0

January 12, 2016
Project Number: 1530704/7000

ATTENTION: Mr. Nick Sawchuk

PROJECT: CSA Concrete Aggregate Testing, December 2015

Sample:	Fine Aggregate
Source:	Sechelt Pit

DATE SAMPLED: December 2015
DATE TESTED: January 6, 2016

SAMPLED BY: Client
TESTED BY: RZ

SIEVE ANALYSIS						
Sieve Size (mm)	% Retained	% Passing	Individual % Retained (Split values)		MATERIAL SPECIFICATION: CSA FA1	
			+ 5	- 5		
10	0.0	100.0	0.0		100	100
5	0.0	100.0	0.0		95	100
2.50	10.3	89.7		10.3	80	100
1.25	17.7	72.0		17.7	50	90
0.630	21.9	50.2		21.9	25	65
0.315	28.6	21.5		28.6	10	35
0.160	16.2	5.3		16.2	2	10
0.080	4.1	1.2		4.1	0	3
PAN	1.2	0		1.2		
Total	100.0		0.0	100.0		

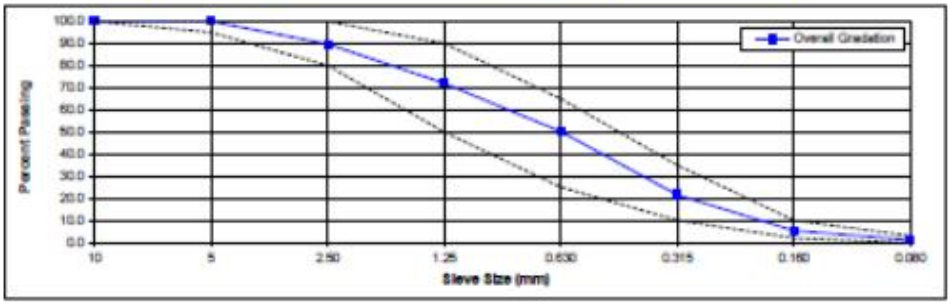

Remarks: Fineness Modulus: 2.61

Reported by: I. Chung

Reviewed by: L. Hu, M.Sc.E., P.Eng.

Notice: The test data given herein pertain to the sample provided, and may not be applicable to material from other production zones/periods. This report constitutes a testing service only. Interpretation of the data given here may be provided upon request.

Appendix: A-II (Coarse aggregates relative density and absorption)

Golder Associates

RELATIVE DENSITY AND ABSORPTION OF COARSE AGGREGATE

CSA A23.2-12A

January 12, 2016
Project Number: 1530704/7000

LEHIGH MATERIALS, DIVISION OF LEHIGH HANSON MATERIALS LTD.
P.O. Box 1790
Sechelt, BC
V0N 3A0

ATTENTION: Mr. Nick Sawchuk

PROJECT: CSA Concrete Aggregate Testing, December 2015

Sample:	**Coarse Aggregate**
Source:	**Sechelt Pit**

Date sampled: December 2015 **Sampled by:** Client
Date tested: January 12, 2016 **Tested by:** DC

Trial No.	Mass (g)	Relative Density (Dry Basis)	Relative Density (SSD Basis)	Apparent Relative Density	Absorption (%)
1	3483.4	2.699	2.717	2.748	0.66
2	3808.0	2.690	2.709	2.743	0.72
AVERAGE		**2.695**	**2.713**	**2.746**	**0.69**

Reported by: I. Chung

Reviewed by: _____
L. Hu, M.Sc.E., P.Eng.

Notice: The test data given herein pertain to the sample provided, and may not be applicable to material from other production zones/periods. This report constitutes a testing service only. Interpretation of the data given here may be provided upon request.

Appendix: A-III (Fine aggregates relative density and absorption)

Golder Associates

RELATIVE DENSITY AND ABSORPTION OF FINE AGGREGATE

CSA A23.2-6A

January 12, 2016
Project Number: 1530704/7000

LEHIGH MATERIALS, DIVISION OF LEHIGH HANSON MATERIALS LTD.
P.O. Box 1790
Sechelt, BC
V0N 3A0

ATTENTION: Mr. Nick Sawchuk

PROJECT: CSA Concrete Aggregate Testing, December 2015

Sample:	**Fine Aggregate**
Source:	**Sechelt Pit**

Date sampled: December 2015 **Sampled by:** Client
Date tested: January 7, 2016 **Tested by:** DC

Trial No.	Mass (g)	Relative Density (Dry Basis)	Relative Density (SSD Basis)	Apparent Relative Density	Absorption (%)
1	500.5	2.649	2.669	2.705	0.79
2	500.8	2.652	2.672	2.708	0.78
AVERAGE		**2.651**	**2.671**	**2.707**	**0.79**

Reported by: I. Chung

Reviewed by: _____
L. Hu, M.Sc.E., P.Eng.

CCIL

Notice: The test data given herein pertain to the sample provided, and may not be applicable to material from other production zones/periods. This report constitutes a testing service only. Interpretation of the data given here may be provided upon request.

Appendix: B - Mix Design Calculations

Concrete

Volume of 1 beam = (L) 350mm x (D) 100mm x (H) 100mm = 3500000 mm^3 = 0.0035 m^3

Volume of 1 cylinder = π x r^2 x h = 0.00157 m^3

As each mix design had 5 cylinders for compression testing and 3 beams for flexural testing, total required volume was calculated to be

Vt= (3 x 0.035) + (5 x 0.00157) = 0.018 m^3

Final volume of batch after adding 15% extra for work losses = 0.018 m^3x 1.15 = 0.021 m^3

Following were the final weights of ingredients used for concrete mix designs;

Cement = 340 Kg/m3 x 0.021 m^3 = 7.18 Kg

Aggregate = 1120 Kg/m3 x 0.021 m^3 = 23.64 Kg

Sand = 820 Kg/m3 x 0.021 m^3 = 17.31 Kg

Water = 181 Kg/m3 x 0.021 m^3 = 3.82 Kg

0.25% fiber = 0.0025 x 0.021 m^3 x 1100 kg/m^3 = 0.058 Kg

0.5% fibers = 0.005 x 0.021 m3 x 1100 kg/m^3 = 0.116 Kg

Mix Design Calculation for Mortar

Volume of 1 briquet = 65786.7 mm3 = 6.57867E-05 m^3

Volume of 1 cube = 125000 m^3 = 0.000125 m^3

Total Volume for 6 briquets and 6 cubes = V_t= (6 x 0.000065) + (6 x 0.000125) = 0.00114 m^3

Final volume of batch after adding 15% extra for work losses = 0.00114 m^3 x 1.15 = 0.00132 m^3

Following were the final weights of ingredients used for concrete mix designs;

Cement = 736 Kg/m^3 x 0.00132 m^3 = 0.97 Kg

Sand = 2207 Kg/m^3 x 0.00132 m^3 = 2.91 Kg

Water = 368 Kg/m^3 x 0.00132 m^3 = 0.48 Kg

0.25% fiber = 0.0025 x 0.00132 m^3 x 1100 kg/m^3 = 0.0036 Kg

0.5% fibers = 0.005 x 0.00132 m^3 x 1100 kg/m^3 = 0.0072 Kg

Appendix: C – Uniaxial Tension Testing Data Graphs

Displacement rates: 2mm/min – CM01, CM02, & CM03, 1.05mm/min – CM04, CM05, CM06

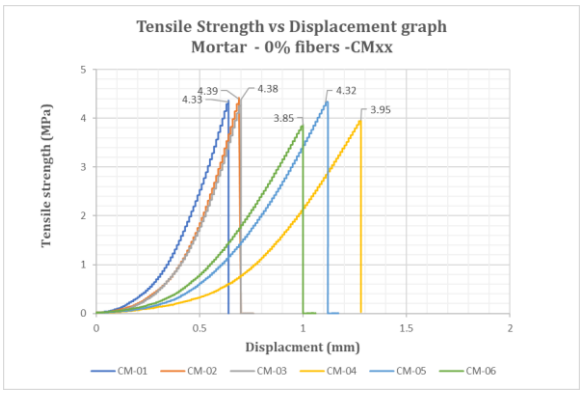

Displacement rates: 1.05mm/min – 0.25M01, 0.25M02, 0.25M03, & 0.48mm/min – 0.25M04, 0.25M05, 0.25M06

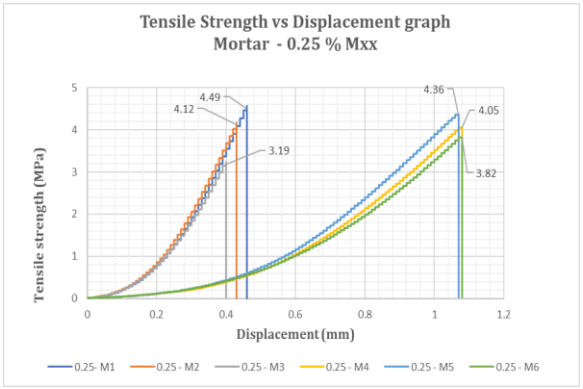

Displacement rates: 1.05mm/min – 0.25M01, 0.25M02, 0.25M03, & 0.48mm/min – 0.25M04, 0.25M05, 0.25M06

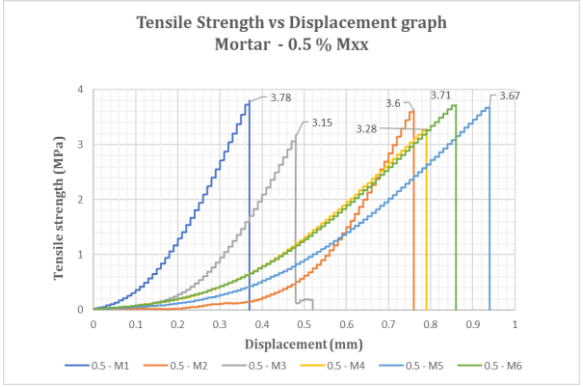

Appendix: D - I: Back Calculation Parameters, Moment Curvature graphs, Load Deflection graphs, Tensile Stress Strain Models, & Compressive Stress Strain Models for CCxx

Modelling Data for CCxx			
Parameters	**CC01**	**CC02**	**CC03**
E	40000	45000	42000
ε_{cr}	0.000095	0.00009	0.00009
α	2.2	2	2.5
γ	1.1	1.25	1.1
η	-0.20833333	-0.35	-0.26666667
μ	0.75	0.65	0.6
b_{tu}	3.5	4	4.4
ω	8.5	7	8.5
λ_{cu}	40	40	40
μ_{crit}	1.023823037	1.05572809	1.023823037

Graphs – CC01

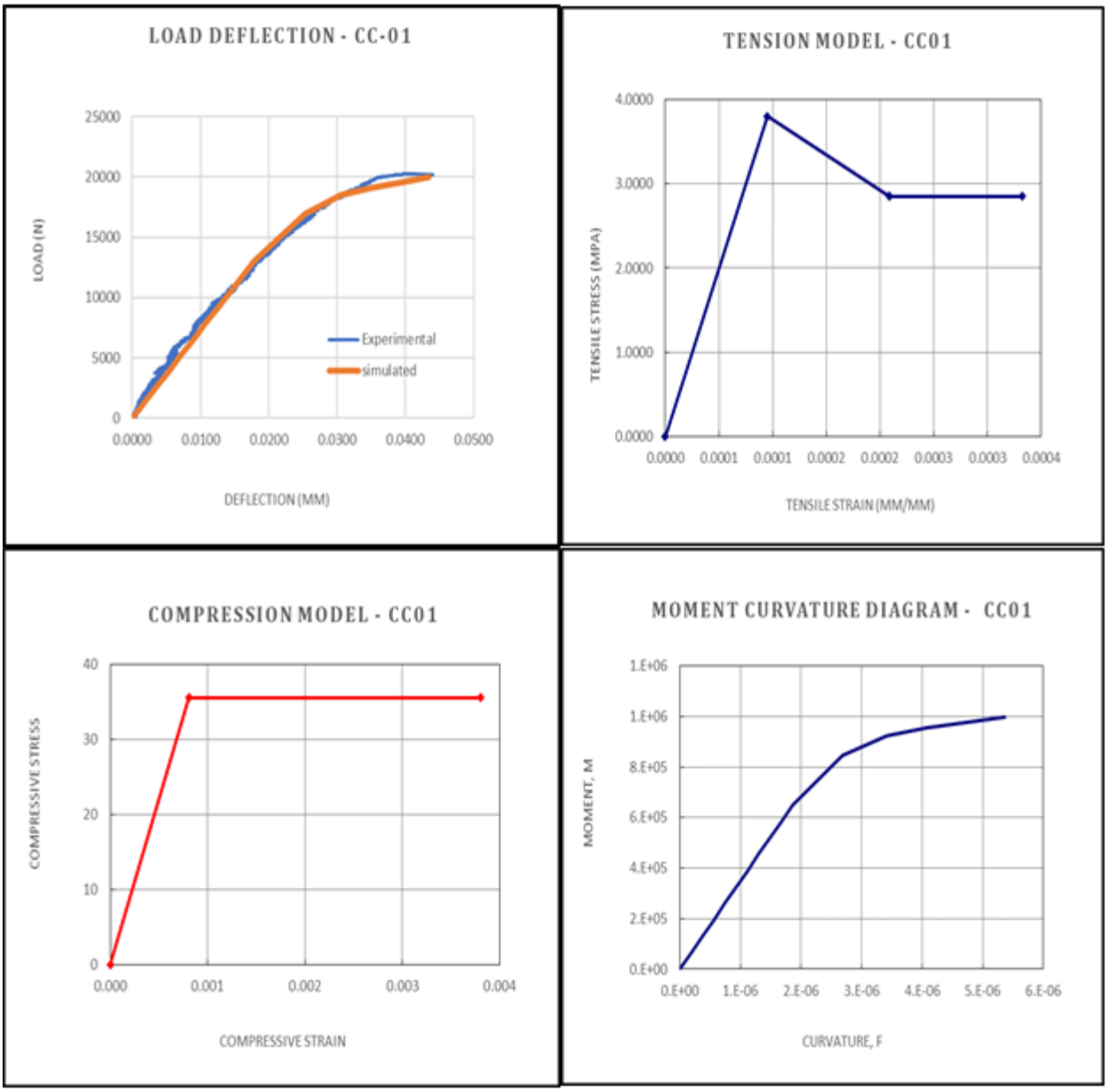

z

Graphs – CC02

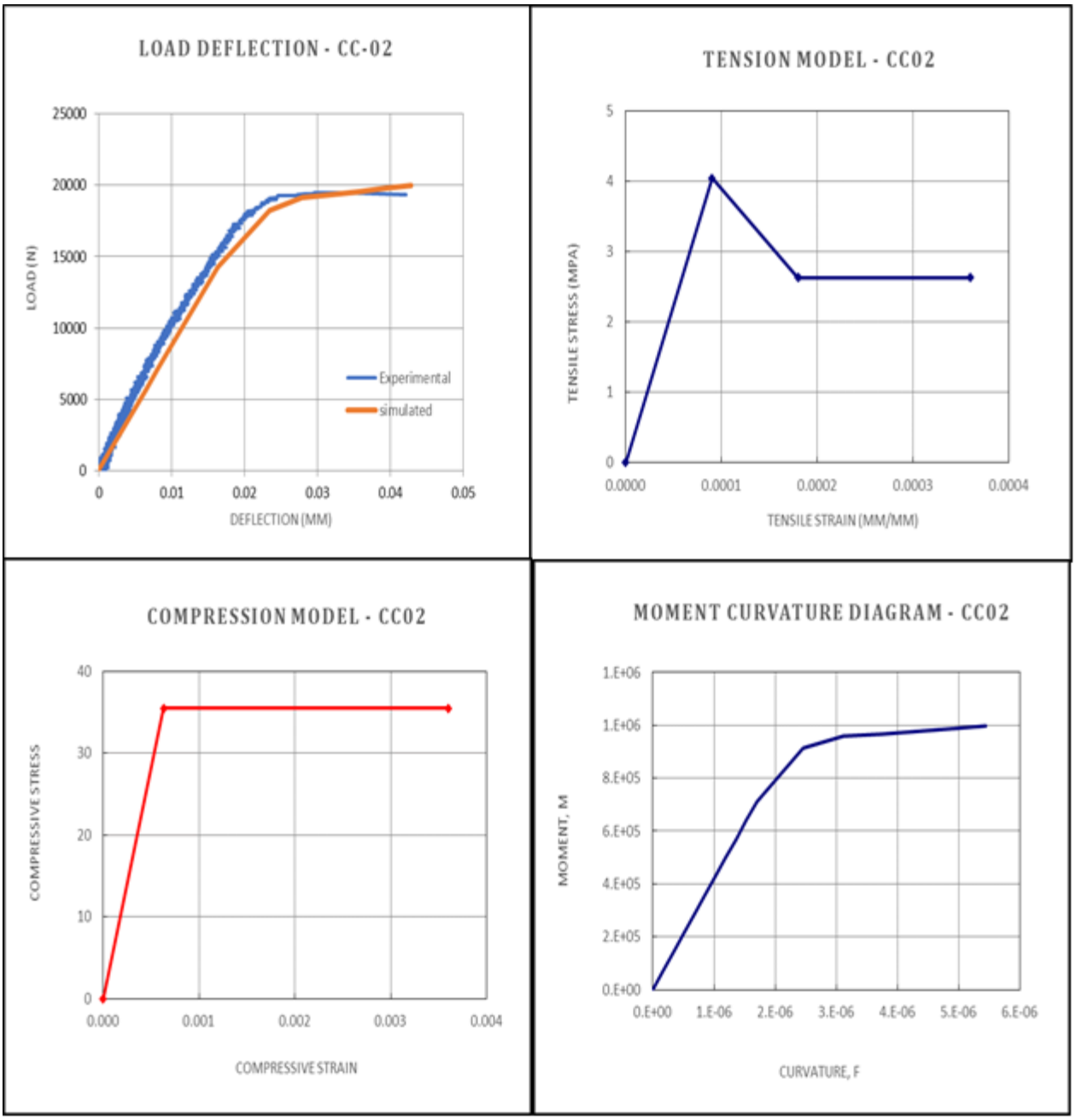
LOAD DEFLECTION - CC-02
LOAD (N)
25000
20000
15000
10000
5000
0
0
0.01
0.02
0.03
0.04
0.05
DEFLECTION (MM)
Experimental
simulated
TENSION MODEL - CC02
TENSILE STRESS (MPA)
5
4
3
2
1
0
0.0000
0.0001
0.0002
0.0003
0.0004
TENSILE STRAIN (MM/MM)
COMPRESSION MODEL - CC02
COMPRESSIVE STRESS
40
30
20
10
0
0.000
0.001
0.002
0.003
0.004
COMPRESSIVE STRAIN
MOMENT CURVATURE DIAGRAM - CC02
MOMENT, M
1.E+06
1.E+06
8.E+05
6.E+05
4.E+05
2.E+05
0.E+00
0.E+00
1.E-06
2.E-06
3.E-06
4.E-06
5.E-06
6.E-06
CURVATURE, F

Graphs – CC03

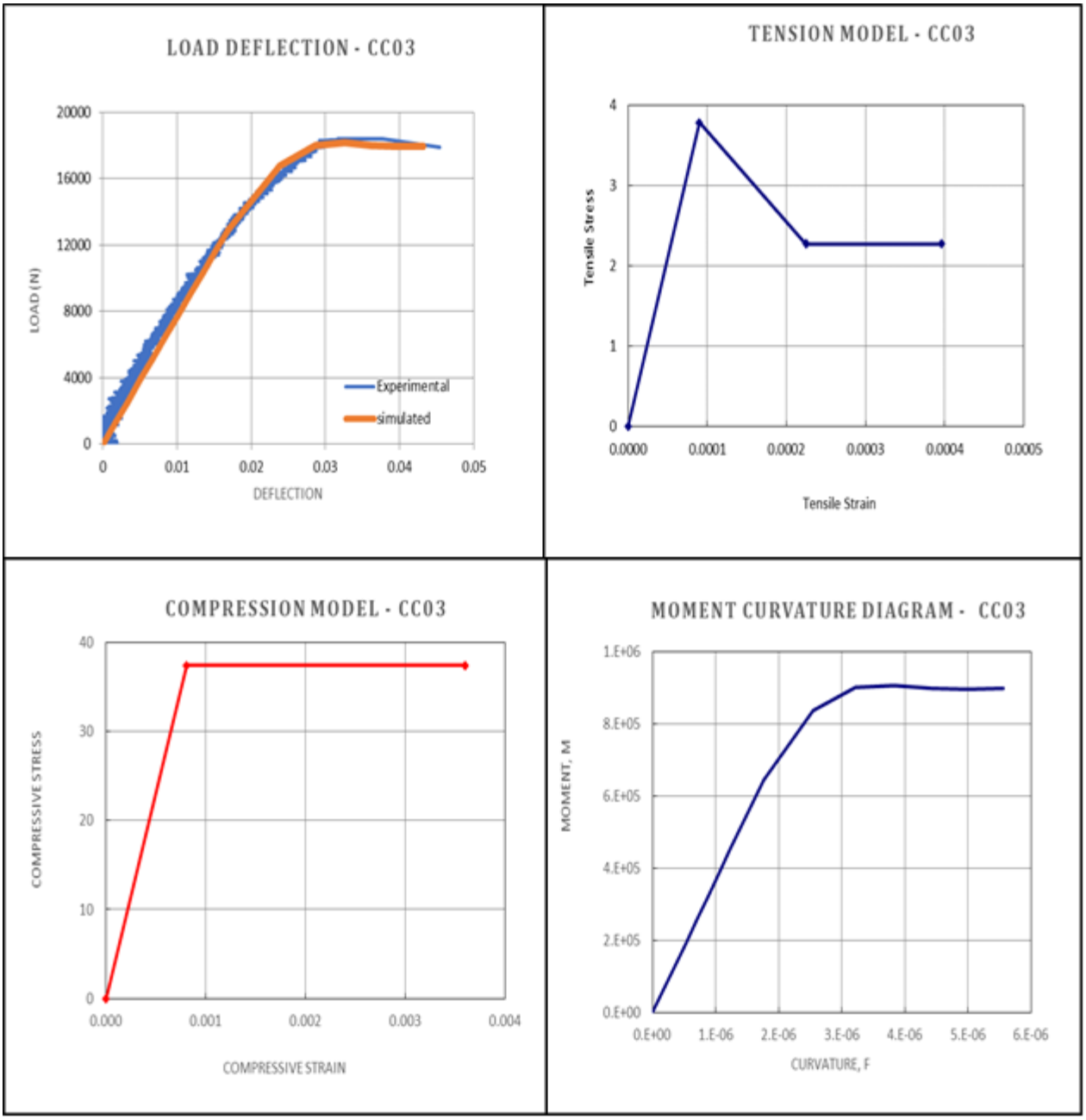
LOAD DEFLECTION - CC03
LOAD (N)
DEFLECTION
Experimental
simulated
TENSION MODEL - CC03
Tensile Stress
Tensile Strain
COMPRESSION MODEL - CC03
COMPRESSIVE STRESS
COMPRESSIVE STRAIN
MOMENT CURVATURE DIAGRAM - CC03
MOMENT, M
CURVATURE, F

Appendix: D-II: Back Calculation Parameters, Moment Curvature graphs, Load Deflection graphs, Tensile Stress Strain Models, & Compressive Stress Strain Models for 0.25%Cxx

Input Data for 0.25%Cxx		
Parameters	**C01**	**C03**
E	26500	29000
Ɛcr	0.0002	0.000165
α	2	2
γ	1	1.25
η	-0.4	-0.4
μ	0.6	0.6
btu	2.5	3
ω	7.15	6.5
λcu	40	40
μcrit	1	1.05572809

Graphs – 0.25%-C01

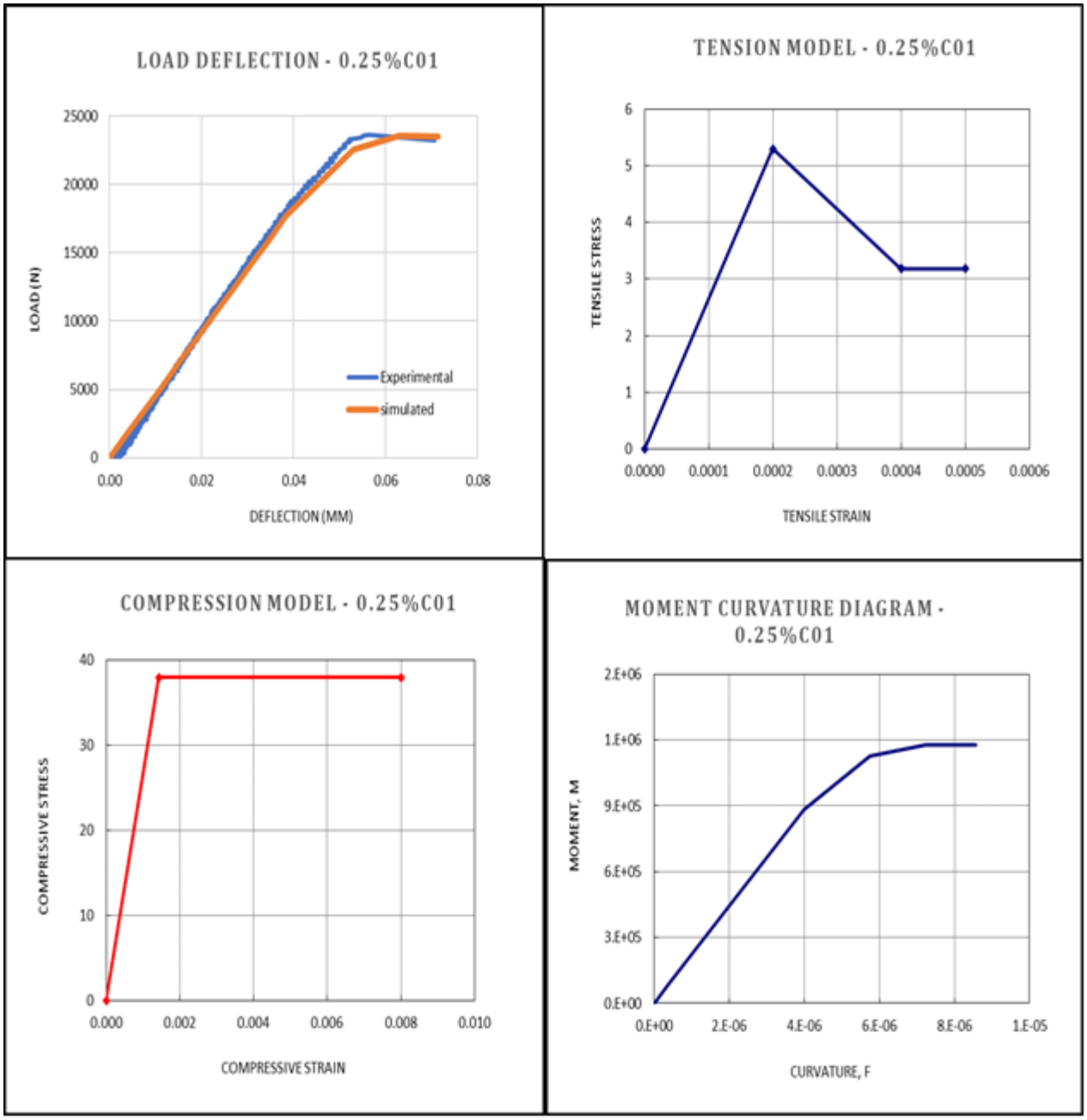

Graphs – 0.25%-C03

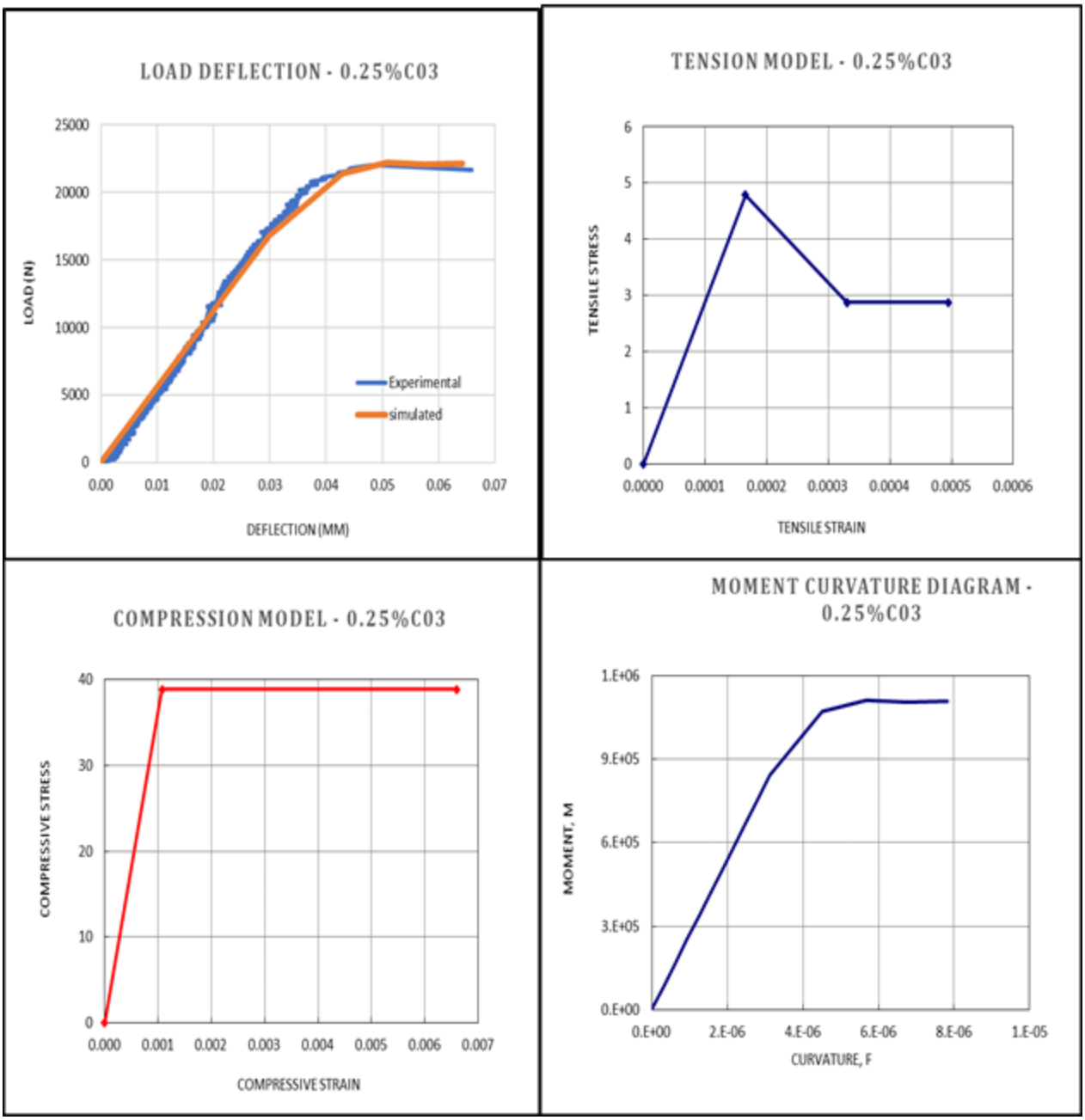

Appendix: D-III: Back Calculation Parameters, Moment Curvature graphs, Load Deflection graphs, Tensile Stress Strain Models, & Compressive Stress Strain Models for 0.5%Cxx

Input Data for 0.5%Cxx			
Parameters	**C01**	**C02**	**C03**
E	30000	37000	33000
ε_{cr}	0.00015	0.000107	0.00013
α	1.4	2	1.2
γ	0.9	1.2	1
η	-0.875	-0.25	-1.75
μ	0.65	0.75	0.65
b_{tu}	2.5	4	3
ω	9.35	7.7	8.8
λ_{cu}	40	40	40
μ_{crit}	0.97367	1.04555	1

Graphs – 0.5%-C02

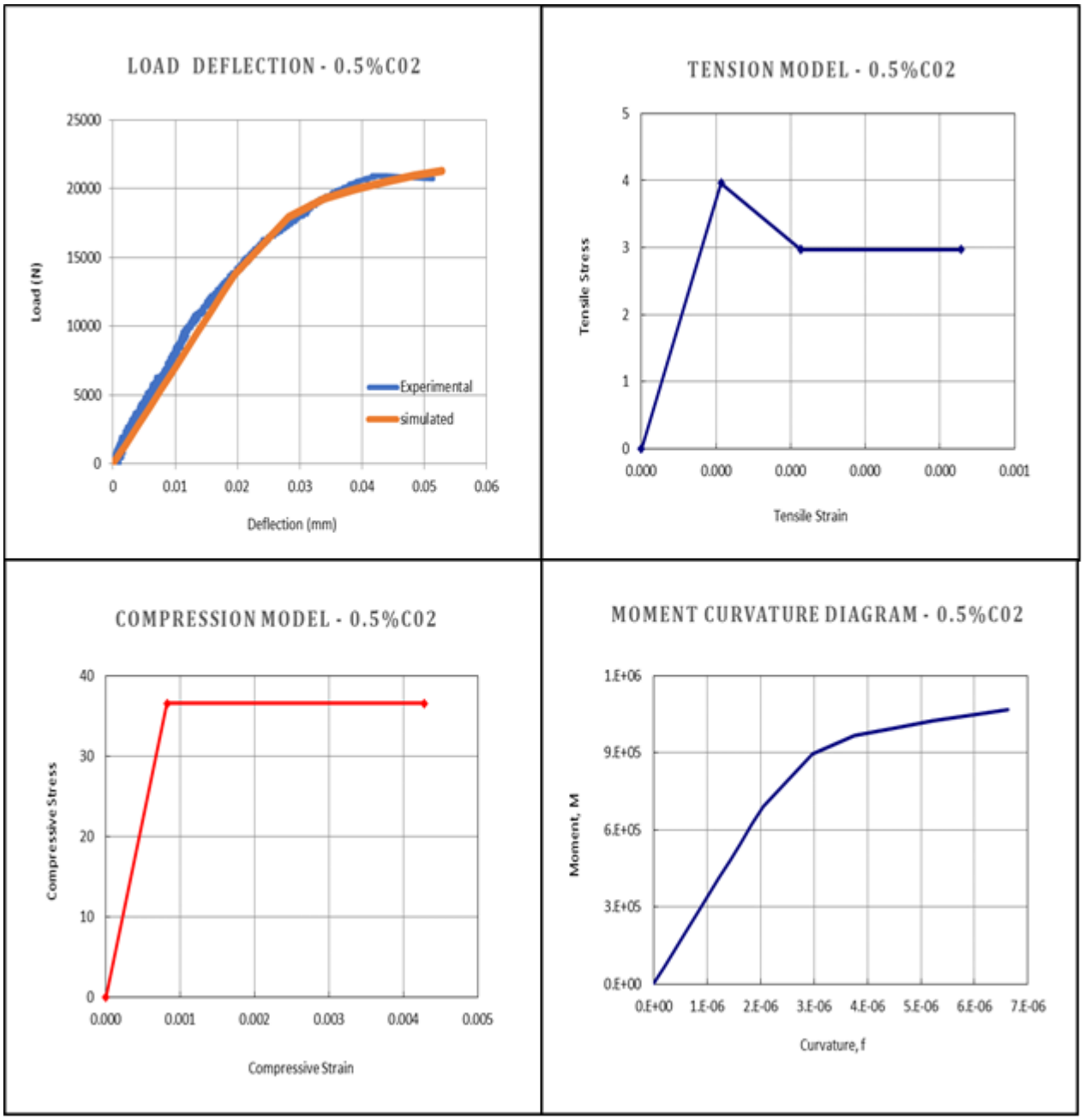

Graphs – 0.5%-C03